1971

Buckling Loads for Partially Embedded Piles

David Allen Wahlstrom

BUCKLING LOADS FOR PARTIALLY EMBEDDED PILES

BY

DAVID ALLEN WAHLSTROM

A thesis submitted
in partial fulfillment of the requirements for the
degree Master of Science, Major in
Civil Engineering, South Dakota
State University

1971

BUCKLING LOADS FOR PARTIALLY

EMBEDDED PILES

This thesis is approved as a creditable and independent investigation by a candidate for the degree, Master of Science, and is acceptable as meeting the thesis requirements for this degree. Acceptance of this thesis does not imply that the conclusions reached by the candidate are necessarily the conclusions of the major department.

Thesis Advisor — Date

Head, Civil Engineering Department — Date

ACKNOWLEDGEMENTS

The research reported herein was performed in the Civil Engineering Department, South Dakota State University, as partial fulfillment of the requirements for the Master of Science degree.

Dr. Peter Y. Lee, Assistant Professor of Civil Engineering, as Advisor, provided immediate supervision and help during the course of the project.

The test apparatus was assembled in the shop of the Civil Engineering Department by Mr. T. Alvin Biggar, who also provided many practical ideas that were incorporated into the equipment and the test procedure.

Professor Emory E. Johnson, Head, Civil Engineering Department, secured funds for the test apparatus and pile specimens. His guidance throughout the last six years was instrumental in prompting the author to return to complete the requirements for the degree.

Professor Ralph H. Davey, Jr., Chairman, Faculty of Civil Technology and Associate Professor Richard T. Tobey, Chairman, Faculty of Humanities, at Sullivan County Community College, South Fallsburg, New York, read the manuscript and

offered helpful suggestions.

Four people were involved in the production of the final manuscript. Assistant Professor L. Jack Agnew, Sullivan County Community College, developed and printed the pictures; Mr. Thomas Ambrosino, Grahamsville, New York, produced the lithographs; and Mr. Warner Mostad, Brookings, South Dakota, drew the figures. The manuscript was typed, proofread, and collated by Miss Rosemary Rosenberger, Hortonville, New York.

The invaluable help and encouragement of these people is greatly appreciated.

TABLE OF CONTENTS

LIST OF TABLES

LIST OF FIGURES

INTRODUCTION

General

Piles are common structural elements used to transmit loads through weak or compressible surface soils to lower, more suitable soil strata. They are relatively small diameter shafts that are forced into the ground. Typical examples of pile utilization can be found at nearly any site where a major structure is being constructed.

Many waterfront structures are built on partially embedded piles. In this case, the pile transfers the load of the structure to the lower soil strata and also serves as a column for the portion of the structure above the mud line. Many bridges and buildings are also supported by partially embedded piles. This is especially true for structures in permafrost areas.

The load bearing capacity of totally embedded and partially embedded piles can usually be determined using readily accepted design procedures. However, the design of partially embedded piles is further complicated by the fact that the column portion of the pile extends below the surface to some point where it can be considered as fixed. It follows, then, that before the design process can proceed, this point of fixity must be defined.

Literature Review

Davisson and Robinson have presented an analytical approach for computing the depth to fixity for a long, partially embedded pile (1). They added this depth to fixity to the unrestrained length to form an equivalent, idealized column. Euler's formula was used to determine the buckling load.

Klohn and Hughes conducted a full scale pile loading test on a timber pile which had an unsupported length of 52 feet (2). A buckling failure was observed and subsequent calculations indicated that the effective length of an equivalent column was 62 feet. Therefore, the depth to fixity was determined to be 10 feet. Davisson, in a discussion of their

paper, has shown that good agreement existed between the test results and the critical load calculated by using the analytical approach set forth by Davisson and Robinson (3).

Lee conducted tests on a number of model piles partially embedded in sand (4). He reported good agreement between the depth to fixity determined experimentally and the depth to fixity predicted by the analytical approach set forth by Davisson and Robinson.

Timoshenko and Gere present a history of, and design formulas for, columns in their book, "Theory of Elastic Stability" (5). They state that for slenderness ratios greater than 105, experimental critical loads agreed very closely with critical loads calculated using Euler's equation.

Rocha stated that for studies in cohesive soils, materials used in models can be the same as the materials of the prototype if the weight can be ignored. In granular soils, the same materials can be used even if weight is a factor (6).

Scope

The analytical approach for determining the depth to fixity can be easily applied to design problems. Once this

depth has been determined, design analysis can proceed utilizing common column design procedures. However, there appear to be no experimental investigations confirming the validity of the analytical method for determining depth to fixity for partially embedded piles in preloaded cohesive soils and only two limited investigations to determine this depth experimentally in noncohesive soils (2 and 4).

In order to attempt to validate the analytical method for determining the depth to fixity for partially embedded piles in preloaded clays, a number of load tests were performed on miniature piles. Tests were also performed on piles partially embedded in a noncohesive soil.

This study is an analysis of these tests.

ANALYTICAL PROCEDURES

The analytical approach for defining the depth to fixity of a partially embedded pile has been presented by Davisson and Robinson (1). The primary features of the partially embedded pile utilized in their paper are shown in Figure 1a. The pile has a length equal to an embedded length, L, plus an unrestrained portion, L_u. The pile may be loaded by an axial load, P, or a moment, M, or a lateral load, Q, or any possible combination of the three. Davisson and Robinson's basic hypothesis was that the partially embedded pile could be idealized by a fixed base column of length, L_e, equal to the unrestrained length, L_u, plus some length equal to the depth to fixity, D_f. Euler's buckling equations are then used to find the critical load for the fixed base column length, L_e. Figure 1b shows the ideal column utilized in these assumptions.

The depth to fixity has been found to be a function of the soils subgrade modulus, k, and the pile stiffness, E I. The

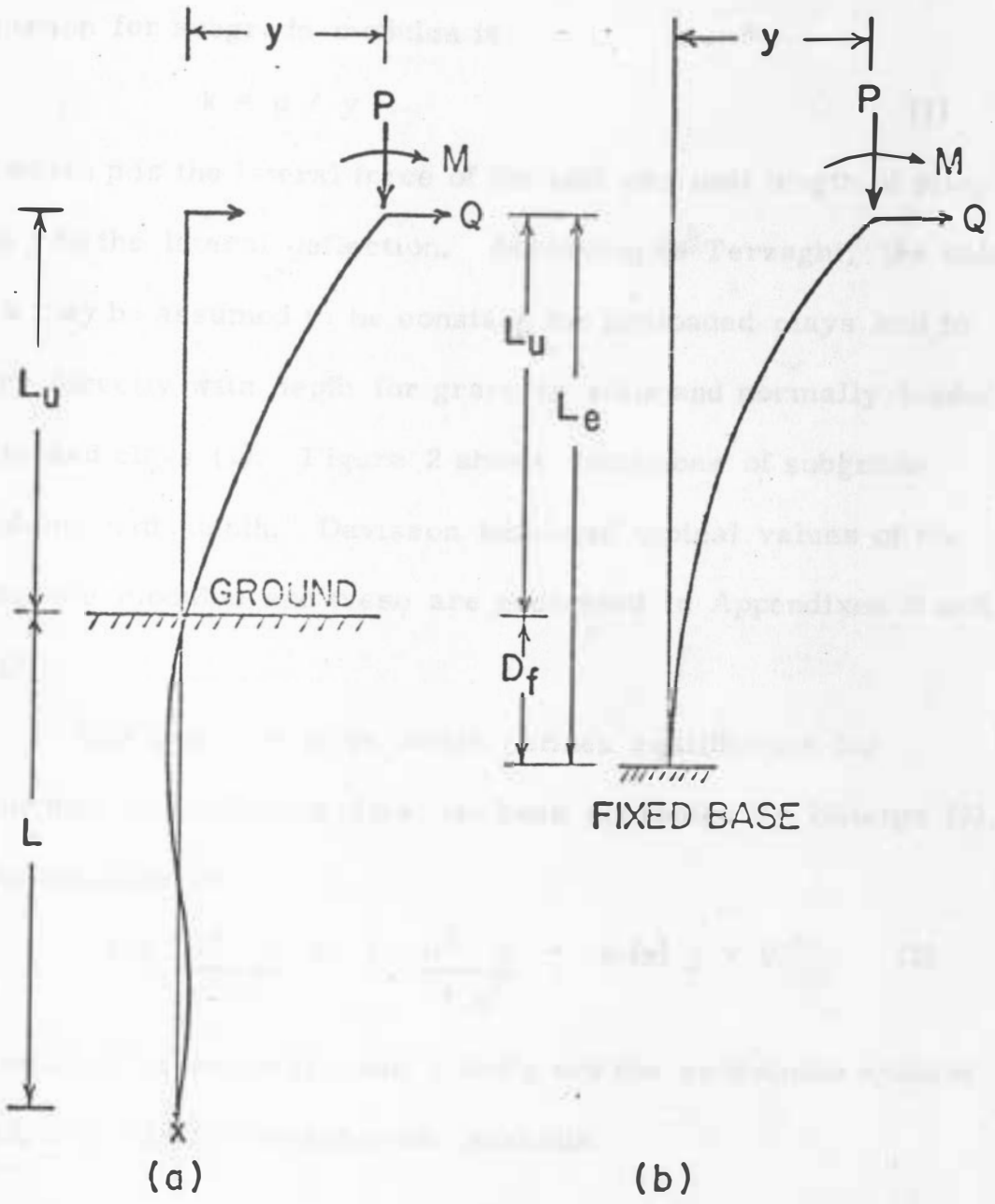

FIGURE 1. PARTIALLY EMBEDDED PILE

equation for subgrade modulus is

$$k = p / y \qquad (1)$$

in which p is the lateral force of the soil per unit length of pile, and y is the lateral deflection. According to Terzaghi, the value of k may be assumed to be constant for preloaded clays and to vary directly with depth for granular soils and normally loaded silts and clays (7). Figure 2 shows variations of subgrade modulus with depth. Davisson tabulated typical values of the subgrade modulus and these are presented in Appendixes B and C (8).

The basic equation which defines equilibrium for embedded and deflected piles has been presented by Hetenyi (9). This equation is

$$E I \frac{d^4 y}{d x^4} + P \frac{d^2 y}{d x^2} + k(x)\, y = 0 \qquad (2)$$

in which P is the axial load; x and y are the coordinate system used; and k (x) is the subgrade modulus.

Preloaded Cohesive Soils

In the analytical approach for defining the depth to fixity for preloaded clays, the applicability of the solutions to Equation 2 become more apparent if the following changes of

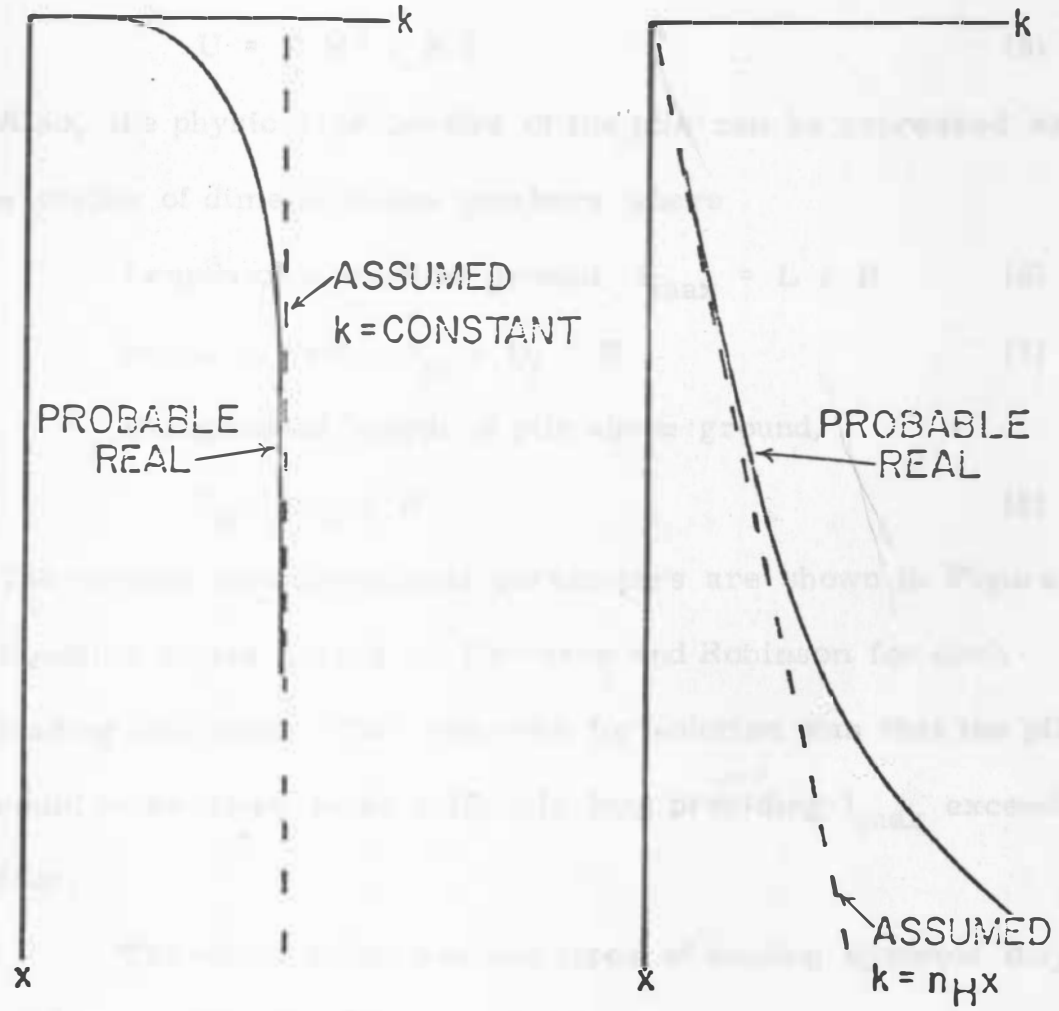

FIGURE 2. VARIATION OF SUBGRADE MODULUS WITH DEPTH

variables are made:

$$R = \sqrt[4]{E I / k} \quad (3)$$

$$F = x / R \quad (4)$$

$$U = P R^2 / E I \quad (5)$$

Also, the physical properties of the pile can be expressed as a series of dimensionless numbers where

Length of pile below ground, $l_{max} = L / R$ (6)

Depth to fixity, $S_R = D_f / R$ (7)

Unsupported length of pile above ground,

$$J_R = L_u / R \quad (8)$$

The various nondimensional parameters are shown in Figure 3. Equation 2 was solved by Davisson and Robinson for each loading condition. The criterion for solution was that the pile could be assumed to be infinitely long providing l_{max} exceeded four.

The effect of the various types of loading systems they investigated resulted in two different stress situations. The lateral load, Q, and the moment, M, create bending stresses; the axial load, P, exerts a buckling force.

The lateral load, Q, or the moment, M, will create a deflection at the free end of the pile equal to y. By solving

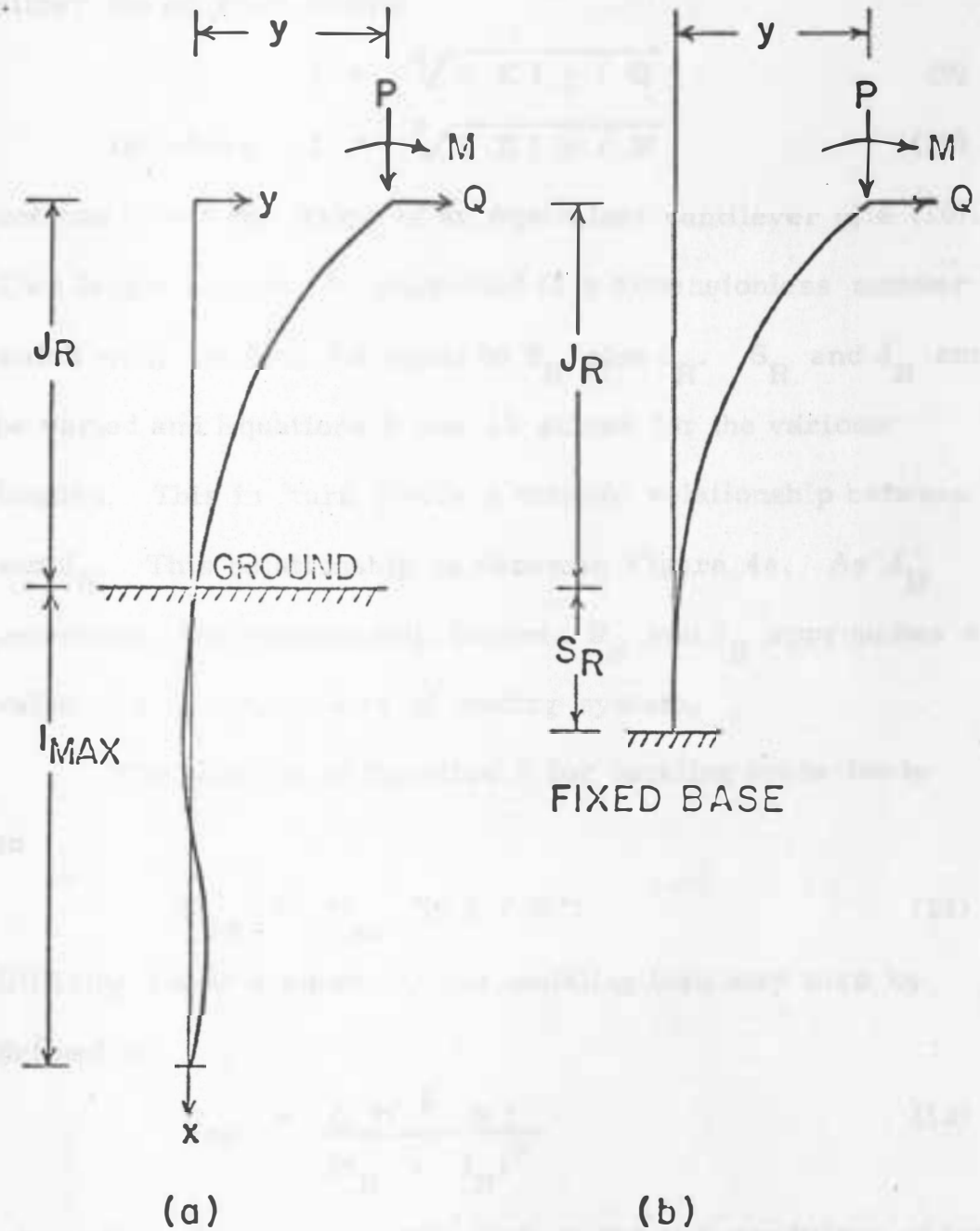

FIGURE 3. NONDIMENSIONAL REPRESENTATION OF PARTIALLY EMBEDDED PILE IN COHESIVE SOIL

either the equation where

$$l = \sqrt[3]{3\,E\,I\,y\,/\,Q} \qquad (9)$$

or where $$l = \sqrt[2]{2\,E\,I\,y\,/\,M} \qquad (10)$$

one can obtain the length of an equivalent cantilever pile (10). This length can then be converted to a dimensionless number which will, in turn, be equal to S_R plus J_R. S_R and J_R can be varied and Equations 9 and 10 solved for the various lengths. This in turn yields a definite relationship between S_R and J_R. This relationship is shown in Figure 4a. As J_R increases, the relationship between S_R and J_R approaches a value of 1.3, regardless of loading system.

The solution of Equation 2 for buckling loads leads to

$$P_{cr} = U_{cr}\ (E\,I\,/\,R^2) \qquad (11)$$

Utilizing Euler's equation, the buckling load may also be defined as

$$P_{cr} = \frac{C\,\pi^2\,E\,I}{(S_R + J_R)^2} \qquad (12)$$

where C is a constant, dependent on the end conditions of the equivalent column (5). By combining Equations 11 and 12, results outlined in Figure 4b are obtained. For values of J_R

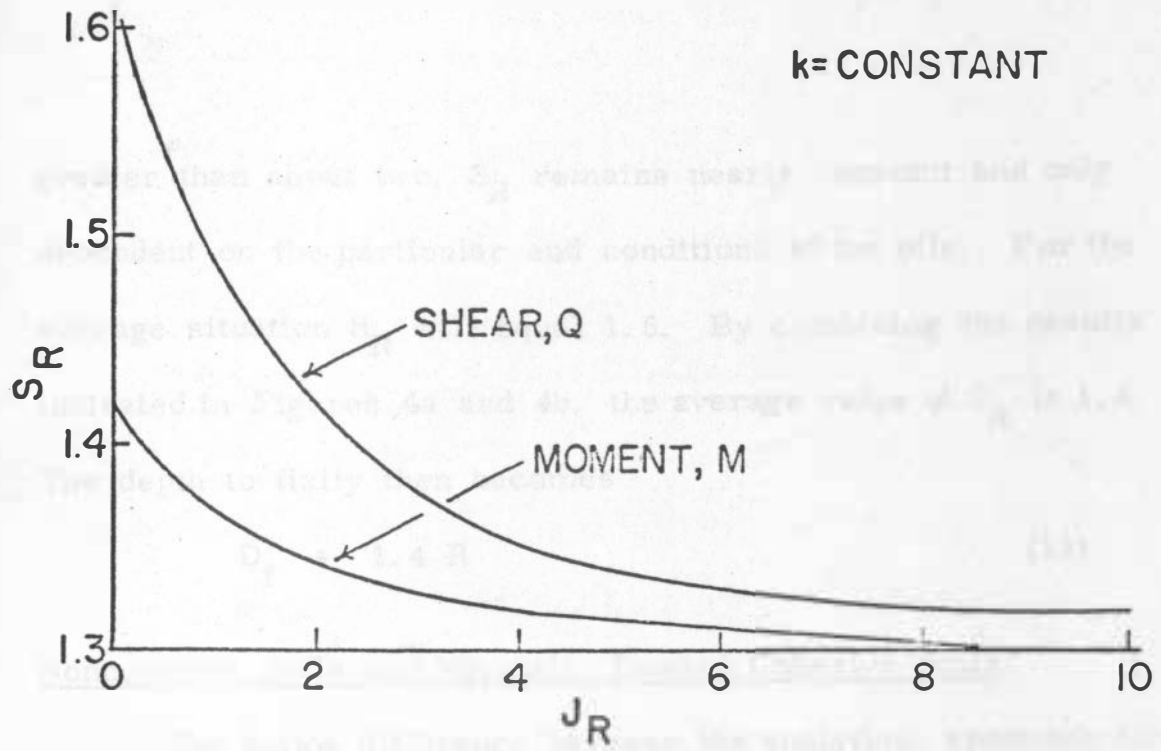

FIGURE 4a. DEPTH TO FIXITY FOR BENDING IN COHESIVE SOIL

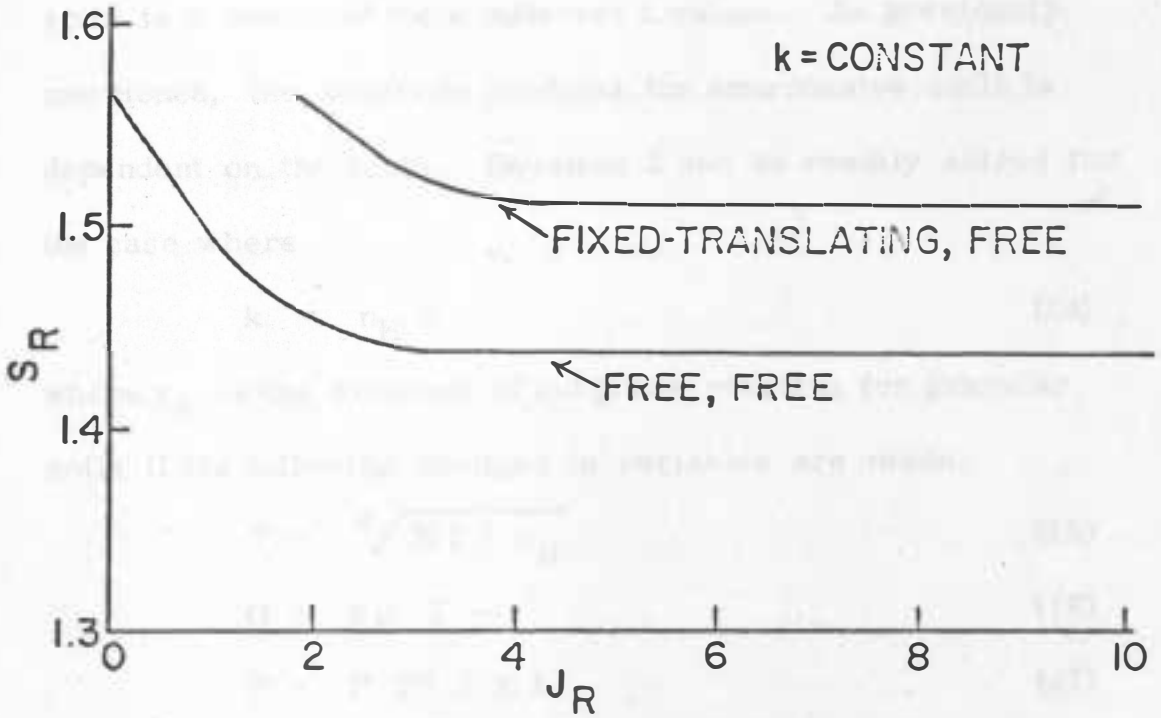

FIGURE 4b. DEPTH TO FIXITY FOR BUCKLING IN COHESIVE SOIL

greater than about two, S_R remains nearly constant and only dependent on the particular end conditions of the pile. For the average situation S_R will equal 1.5. By combining the results indicated in Figures 4a and 4b, the average value of S_R is 1.4. The depth to fixity then becomes

$$D_f = 1.4\ R \tag{13}$$

Noncohesive Soils and Normally Loaded Cohesive Soils

The major difference between the analytical approach for preloaded clay soils and the analytical approach for granular soils is a result of their different k values. As previously mentioned, the subgrade modulus for noncohesive soils is dependent on the depth. Equation 2 can be readily solved for the case where

$$k = n_H\ x \tag{14}$$

where n_H is the constant of subgrade reaction for granular soils if the following changes in variables are made:

$$T = \sqrt[5]{E\ I\ /\ n_H} \tag{15}$$

$$G = x\ /\ T \tag{16}$$

$$V = P\ T^2\ /\ E\ I \tag{17}$$

Also, the physical properties of the pile can be expressed as a

series of dimensionless numbers where

Length of pile below ground, $z_{max} = L / T$ (18)

Depth to fixity, $S_T = D_f / T$ (19)

Unsupported length of pile above ground,

$$J_T = L_u / T \quad (20)$$

This series of nondimensional parameters is shown in Figure 5.

The solution of Equation 2 for each loading condition, assuming that z_{max} exceeds four, leads to the relationship between S_T and J_T expressed in Figures 6a and 6b.

The various loads, Q, M, and P create types of stress similar to those in preloaded cohesive soils - the lateral load, Q, and the moment, M, create bending stresses; the axial load, P, creates a buckling load.

When the stress results from bending and J_T exceeds four, S_T can be assumed to equal approximately 1.75. When the stress results from buckling and J_T exceeds three, S_T equals 1.8. A comparison of the bending and buckling results shows that the conservative value of S_T is 1.8. Therefore, the depth to fixity becomes

$$D_f = 1.8 \ T \quad (21)$$

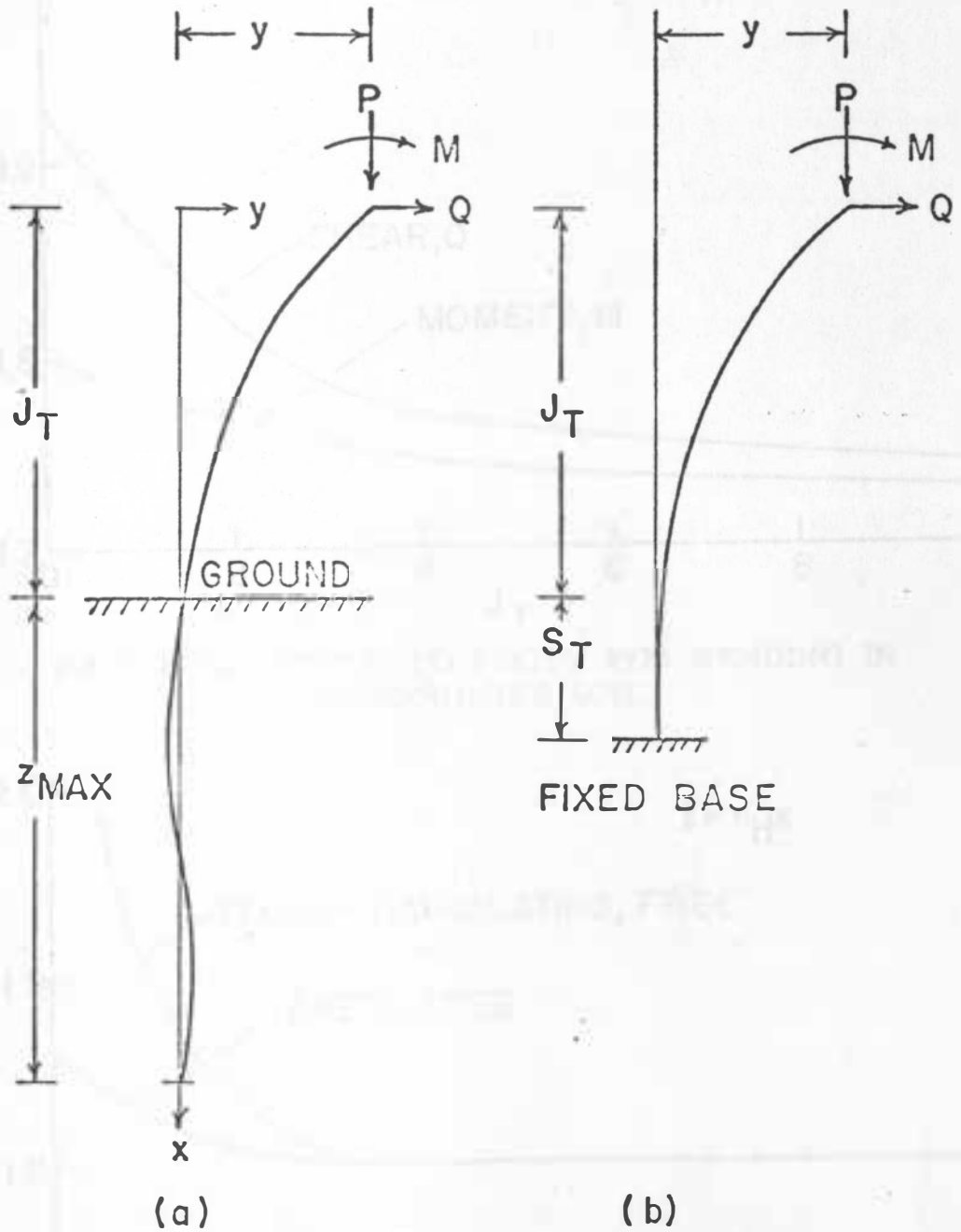

FIGURE 5. NONDIMENSIONAL REPRESENTATION OF PARTIALLY EMBEDDED PILE IN NONCOHESIVE SOIL

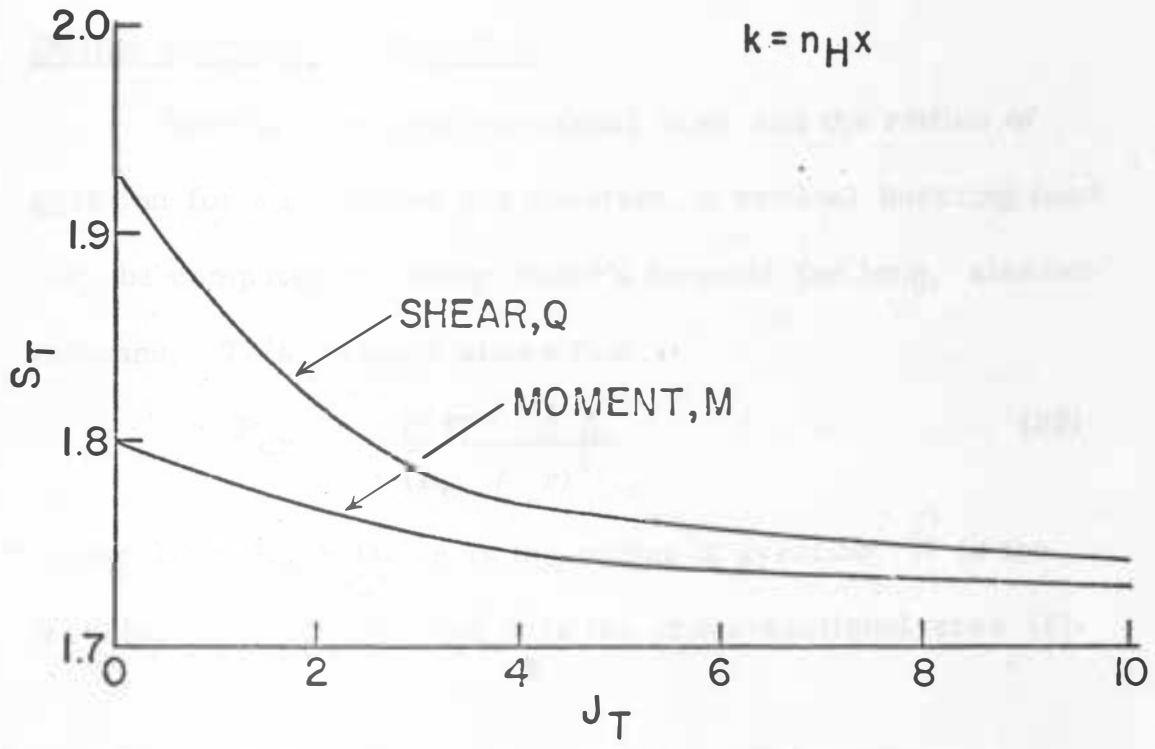

FIGURE 6a. DEPTH TO FIXITY FOR BENDING IN NONCOHESIVE SOIL

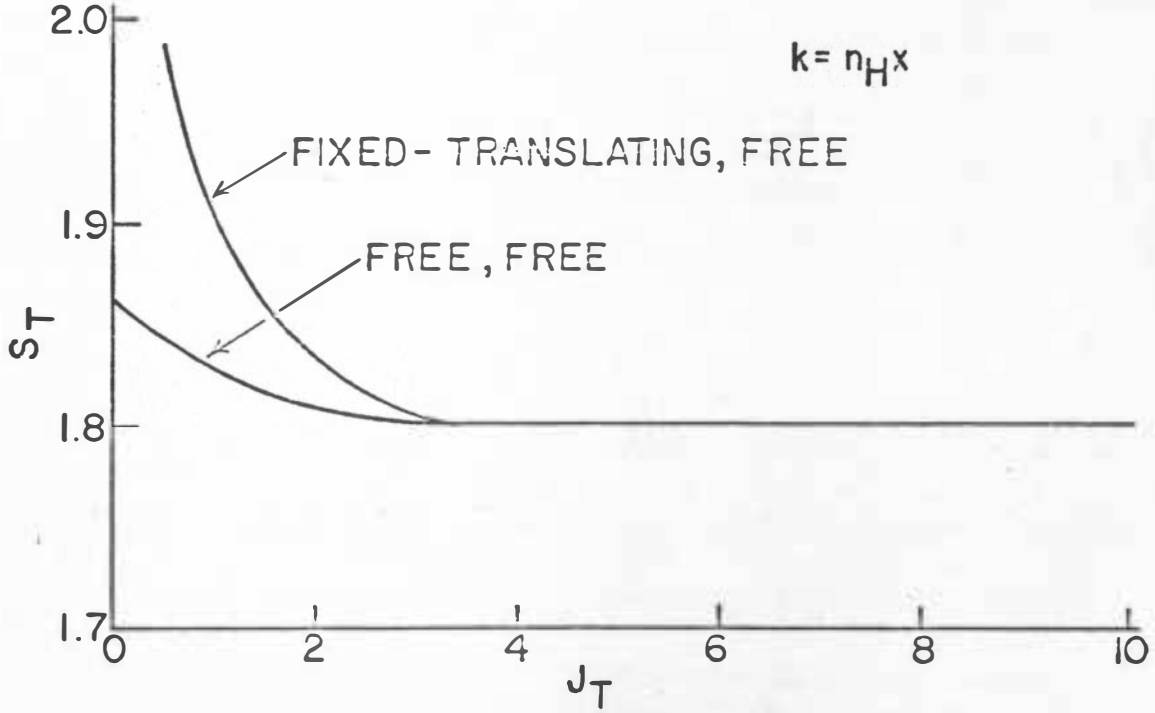

FIGURE 6b. DEPTH TO FIXITY FOR BUCKLING IN NONCOHESIVE SOIL

Design Formula for Buckling

Because the cross-sectional area and the radius of gyration for a specimen are constant, a critical buckling load may be computed by using Euler's formula for long, slender columns. This formula states that

$$P_{cr} = \frac{C \pi^2 E A}{(L_e / r)^2} \qquad (22)$$

where $L_e = L_u + D_f$, r is the radius of gyration, E is the modulus of elasticity, and A is the cross-sectional area (5).

EXPERIMENTAL INVESTIGATIONS

Loading tests to determine buckling loads were performed on thirty-five model piles. The model piles consisted of steel and copper specimens having tubular, rectangular, or circular cross-sections. Table 1 lists the various physical properties of the test specimens.

Subgrade Modulus

An integral part of the analytical considerations for determining depth to fixity is the k value of the particular soil. Before predicted critical loads could be determined, it was necessary to determine the k value.

Experimental Determination of k

The first series of tests were performed in a cohesive soil. Classification data for the clay used in this investigation are included in Appendix D. Because the soil was recompacted for each test, it was almost impossible to maintain

TABLE 1. PHYSICAL PROPERTIES OF MODEL PILE SPECIMENS

Specimen	Length in inches	Outside diameter in inches	Inside diameter in inches	I in inches^4	E in pounds per inch^2	E I in pound - inches^2
3/16 inch steel rod	48	0.1875	--	0.000061	30×10^6	1820.1
1/4 inch steel rod	48	0.25	--	0.000192	30×10^6	5752.4
5/16 inch steel rod	48	0.3125	--	0.000468	30×10^6	14044.0
3/8 inch steel rod	48	0.376	--	0.000977	30×10^6	29322.0
1/4 inch steel bar	48	1.0 (width)	0.25 (thickness)	0.001302	30×10^6	39062.5
1/8 inch steel pipe	48	0.402	0.272	0.001013	30×10^6	30383.6
1/2 inch copper pipe	48	0.627	0.567	0.002506	16.5×10^6	41348.6

identical density and moisture conditions in consecutive tests. Therefore, it was necessary to determine k for each test. This was done using the loading apparatus shown in Figure 7. The procedures employed were a modification of those suggested by Terzaghi for field tests (7).

The test apparatus was a solid 7/8-inch square, 42-inch long steel bar embedded in the soil to a depth equal to L for the model pile being tested. The bottom end was restrained in a ball-and-socket arrangement and a load, Q, was applied to the upper end of the bar.

When a lateral load was applied to the top of the bar, a resisting pressure developed in the soil. Figure 8b shows the anticipated soil reaction from a lateral load. The deflection of the top of the bar, y_1, was measured for each load, Q. Figure 9 shows a graph of a typical load vs deflection test. Summing moments about the pivot leads to the equation:

$$k = \frac{3\ (H + H_1)\ (H + H_2)}{H^3}\ \frac{Q}{y_1} \qquad (23)$$

where H, H_1, and H_2 are as shown in Figure 8a; and Q is a load at some deflection, y_1.

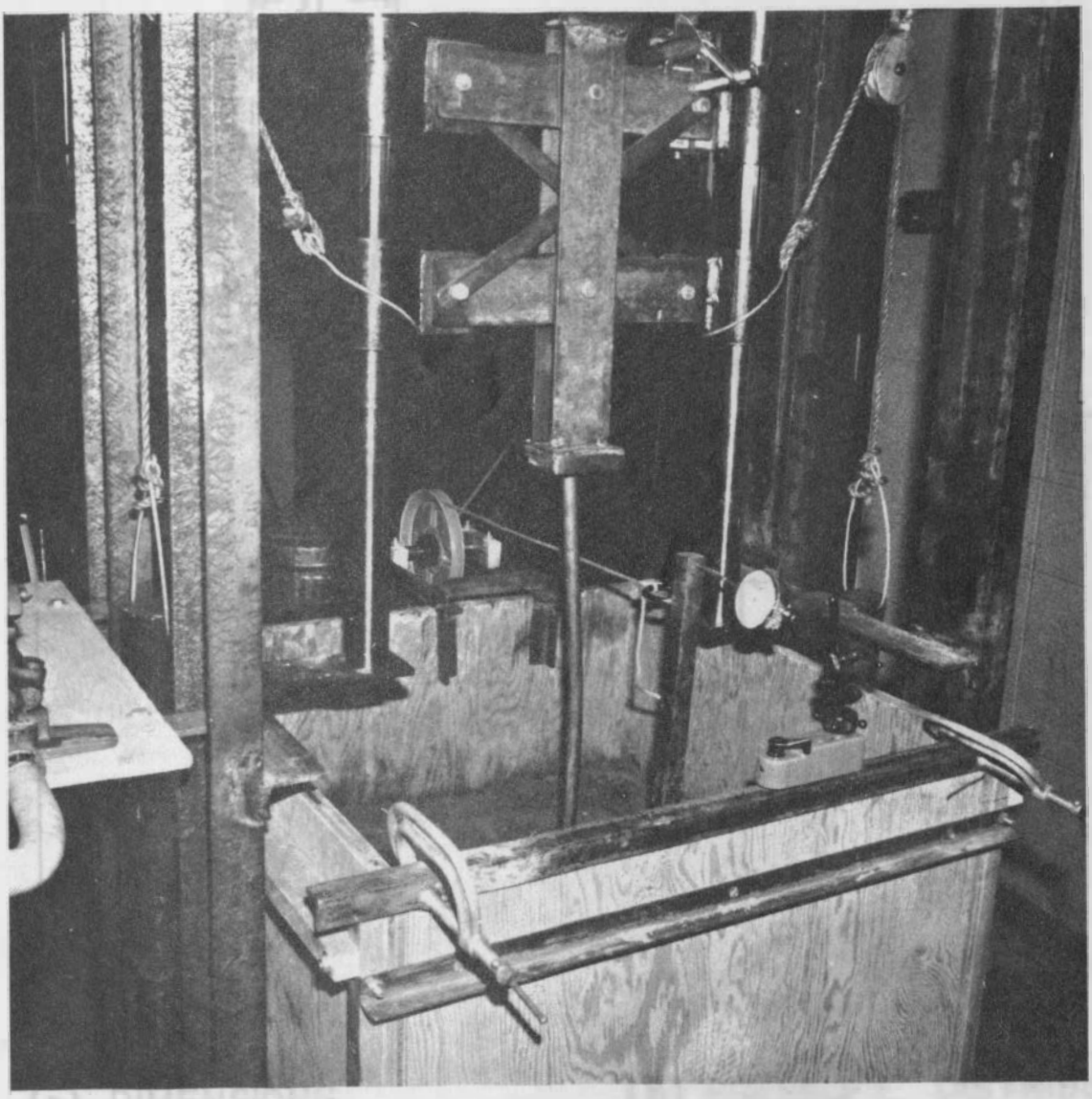

FIGURE 7. TEST TO DETERMINE SUBGRADE MODULUS

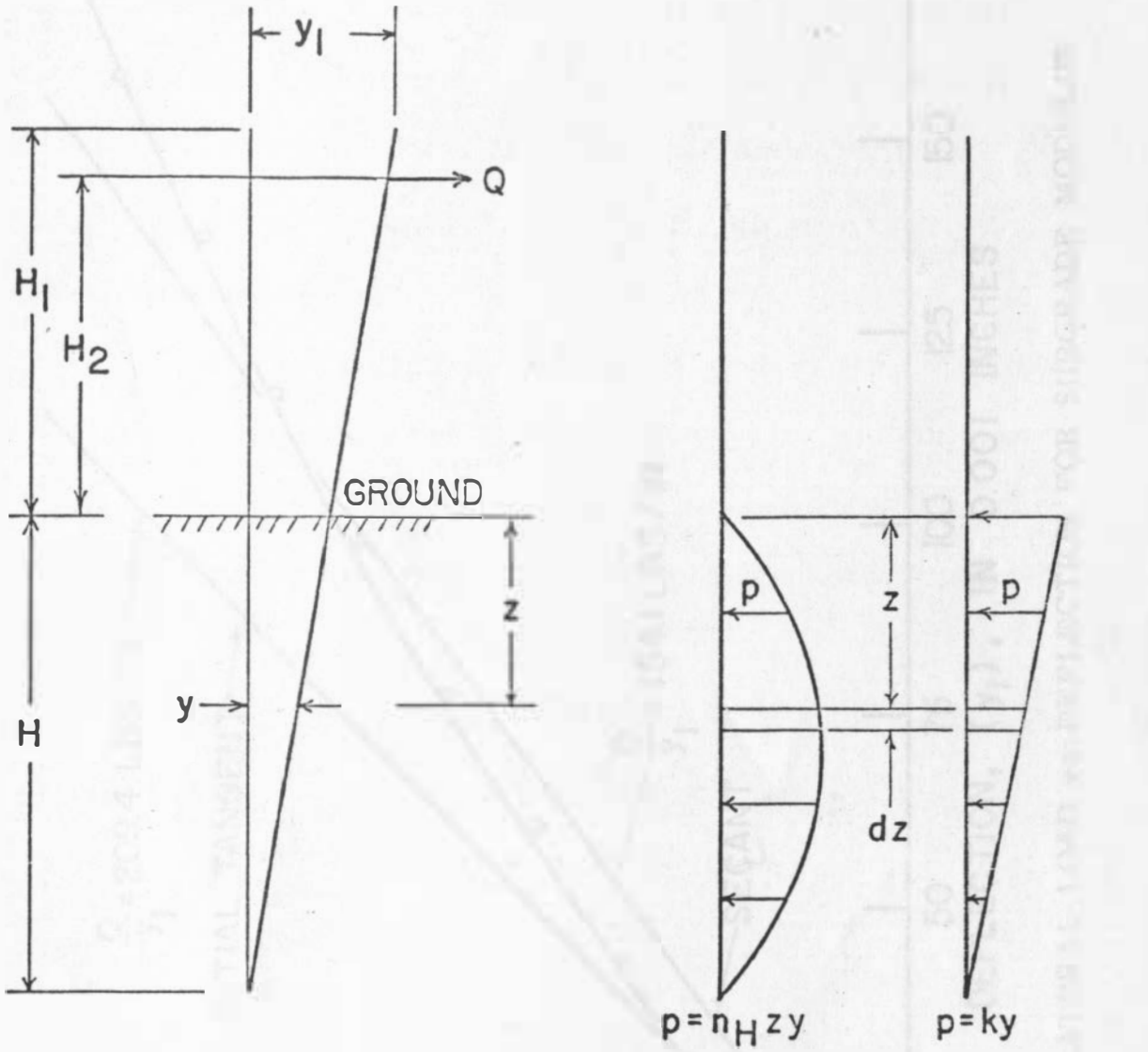

FIGURE 8. SUBGRADE MODULUS DETERMINATIONS

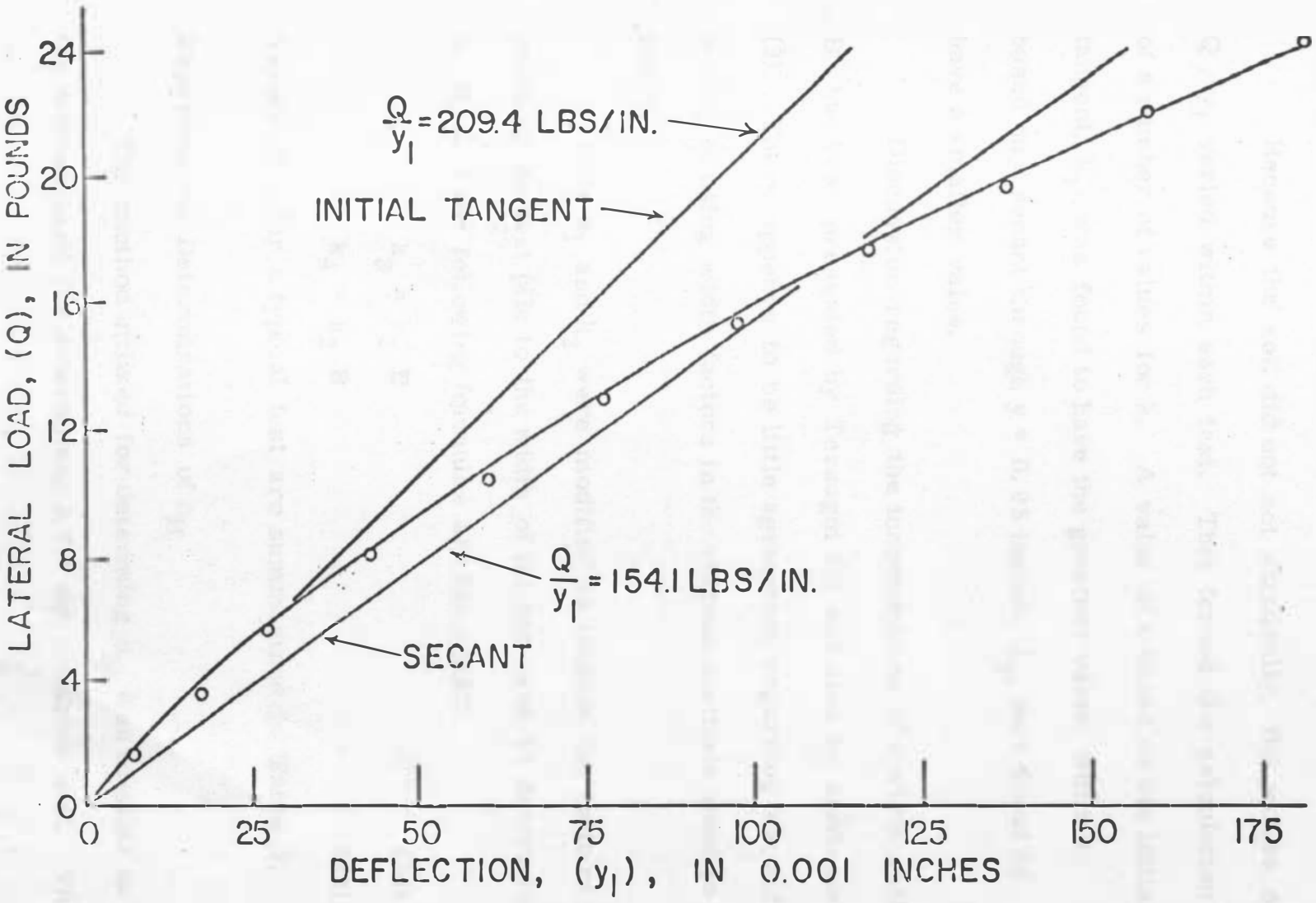

FIGURE 9. LATERAL LOAD vs DEFLECTION FOR SUBGRADE MODULUS

Because the soil did not act elastically, the values of Q / y_1 varied within each test. This forced the calculation of a number of values for k. A value of k based on the initial tangent, k_1, was found to have the greatest value, while k based on a secant through y = 0.05 inches, k_2, was found to have a smaller value.

Discussion regarding the incorporation of a width ratio, B, has been presented by Terzaghi (7) and also by Davisson (3). There appears to be little agreement regarding the suitability of using width factors in the various methods used to find k.

Both k_1 and k_2 were modified to include the ratio of the width of the test pile to the width of the bar used to determine k, B, and the following formulas are the result:

$$k_3 = k_1 B \tag{24}$$

$$k_4 = k_2 B \tag{25}$$

Values of k for a typical test are summarized in Table 2.

Experimental Determinations of n_H

The method utilized for determing n_H was similar to the method used for determining k for the cohesive soil. The

TABLE 2. TYPICAL VALUES OF k FOR THE CLAY

Specimen	k_1 in pounds per inch^2	k_2 in pounds per inch^2	k_3 in pounds per inch^2	k_4 in pounds per inch^2
3/8 inch steel rod	147.8	79.1	63.4	33.9
1/2 inch copper pipe	167.2	105.4	119.9	75.6
1/4 inch steel bar	191.7	97.7	219.1	111.7

apparatus used was identical. It was easier to maintain consistent densities because the granular soil was dry and was not compacted. Therefore, it was only necessary to conduct one series of tests to determine n_H. Modification of Equation 23 for granular soils results in

$$n_H = \frac{12 \ (H + H_1)}{H^4} \frac{(H + H_2)}{y_1} \frac{Q}{} \qquad (26)$$

The values of n_H are summarized in Table 3. A value of n_H equal to 15.6 pounds per inch^3 was used in the theoretical calculations. This is somewhat higher than the value of n_H = 8 pounds per inch^3 suggested for a loose sand, but less than the suggested value of n_H = 24 pounds per inch^3 for a medium dense sand (3). Classification data for the sand used in this investigation are included in Appendix E.

Loading Tests on the Model Piles

Loading tests were conducted on thirty-five model pile specimens. The loading device was a specially designed machine which was capable of exerting an axial load in excess of 5000 pounds. It consisted of a box 2 ft x 2 ft x 3 ft and a loading frame. Figure 10 shows the machine with a test specimen in place. Figure 11 shows the arrangement of the

TABLE 3. VALUES OF n_H FOR SAND

Test number	H in inches	n_H in pounds per inch
1	12.0	24.6
2	15.75	16.4
3	24.13	14.9

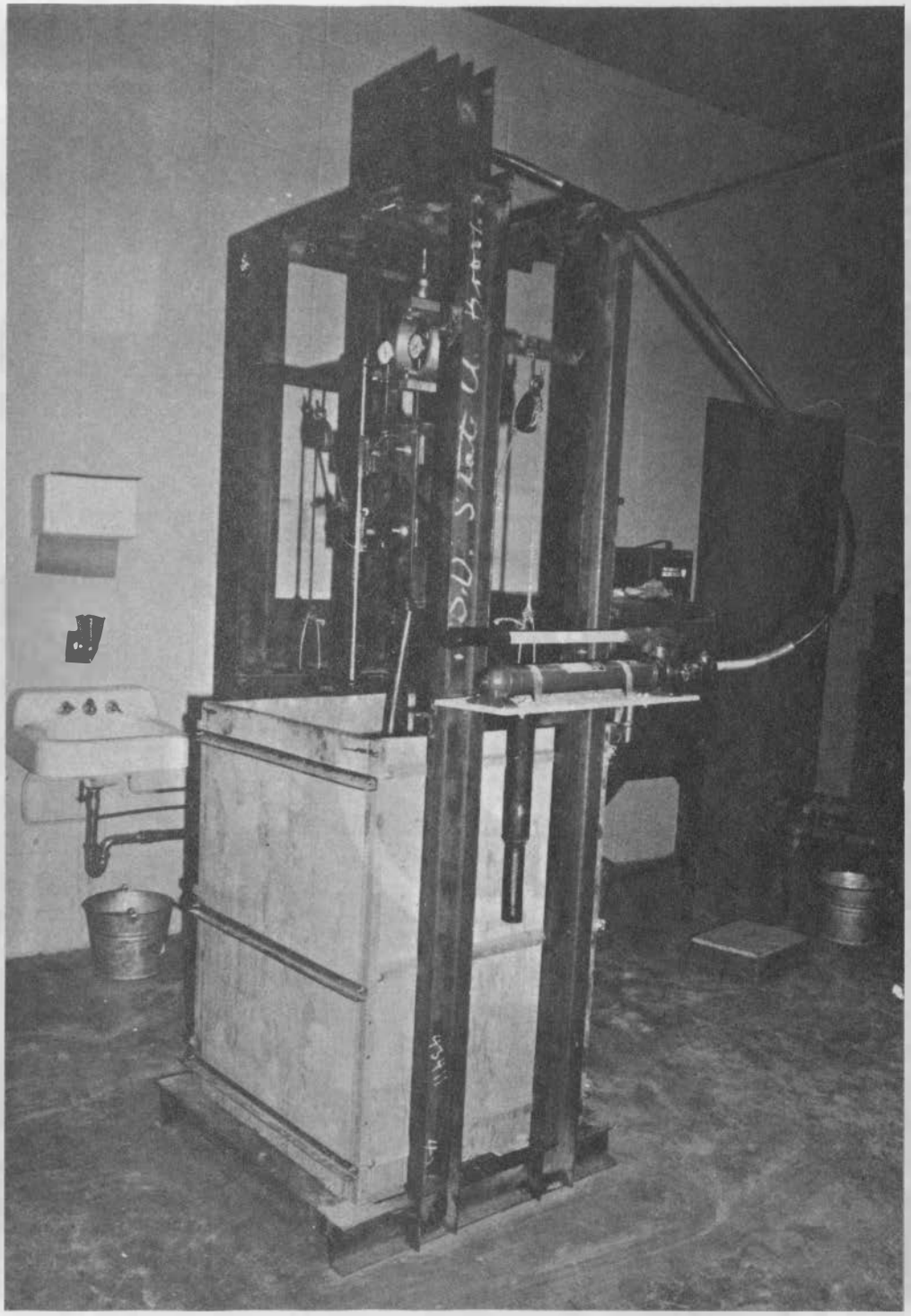

FIGURE 10. PILE LOADING APPARATUS

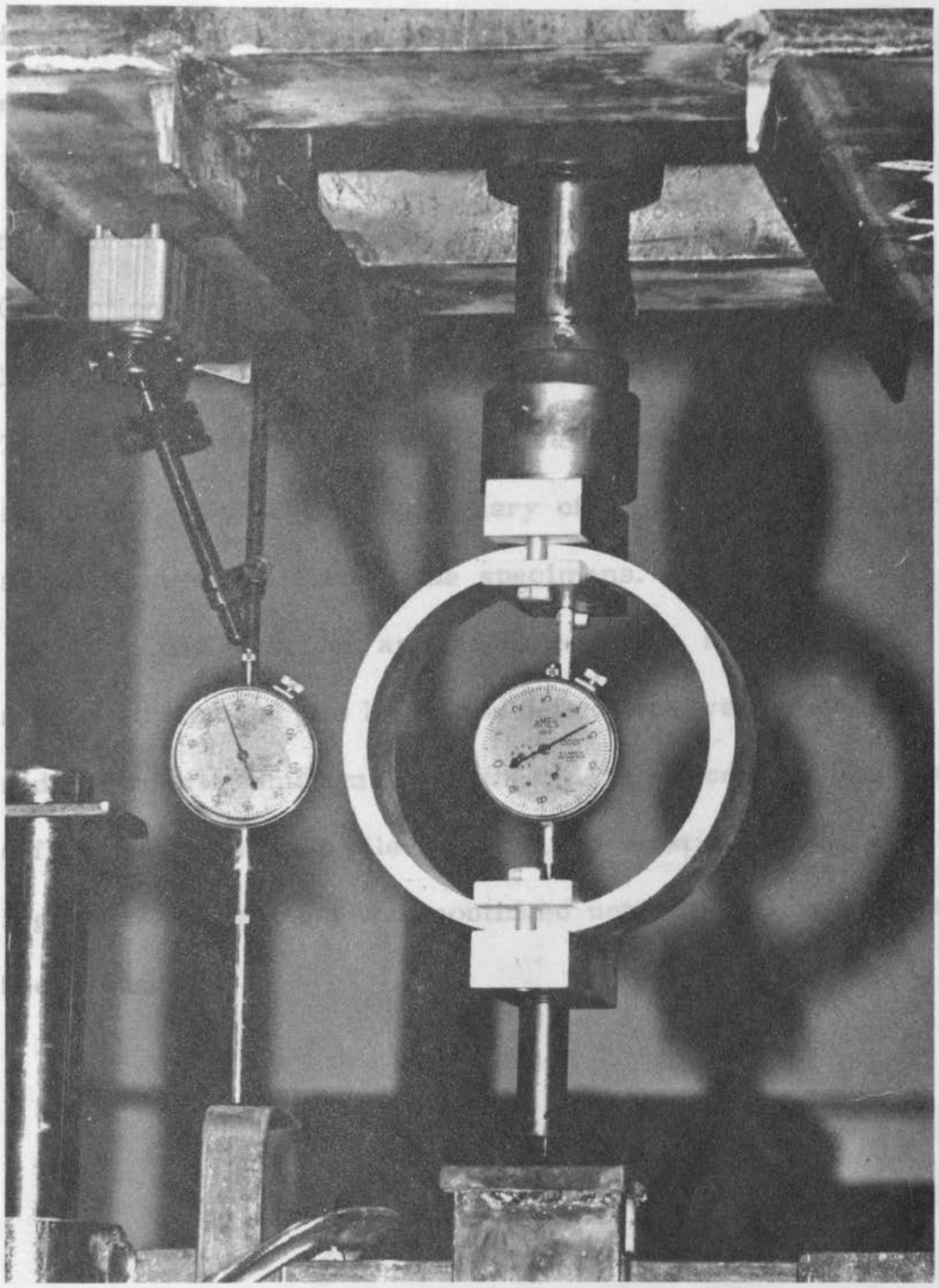

FIGURE 11. DEFLECTION GAGE AND PROVING RING

proving ring which was used to measure loads and the deflection gage which was used to measure compression of each test specimen.

Before loading, the modulus of elasticity, E, and the moment of inertia, I, were determined for each specimen. Calculations were then made to insure compliance with the limitations established for Equations 6, 8, 18, and 20. Table 1 is a summary of the physical properties of the pile specimens. Table 4 is a summary of the range of nondimensional parameters for the pile specimens.

A load was then applied to each pile at a controlled rate of strain; and pile loads and deflections were measured and recorded at uniform intervals. A representative load vs deflection graph for a pile which failed elastically is shown in Figure 12. Each test was continued until the failing load had been reached.

TABLE 4. VALUES OF NONDIMENSIONAL PARAMETERS

Specimen	k = constant		k = $n_H x$	
	l_{max}	J_R	z_{max}	J_T
3/16 inch steel rod	11.10	10.39 to 15.87	--	--
1/4 inch steel rod	--	--	5.89 to 8.56	6.12 to 8.79
5/16 inch steel rod	--	--	6.17 to 6.33	6.01 to 6.17
3/8 inch steel rod	5.30 to 6.13	6.46 to 7.89	--	--
1/4 inch steel bar	5.59 to 5.79	6.47 to 6.91	--	--
1/8 inch steel pipe	5.41 to 6.60	5.00 to 7.59	4.73 to 5.33	5.22 to 5.82
1/2 inch copper pipe	5.24 to 5.53	6.88 to 7.11	--	--

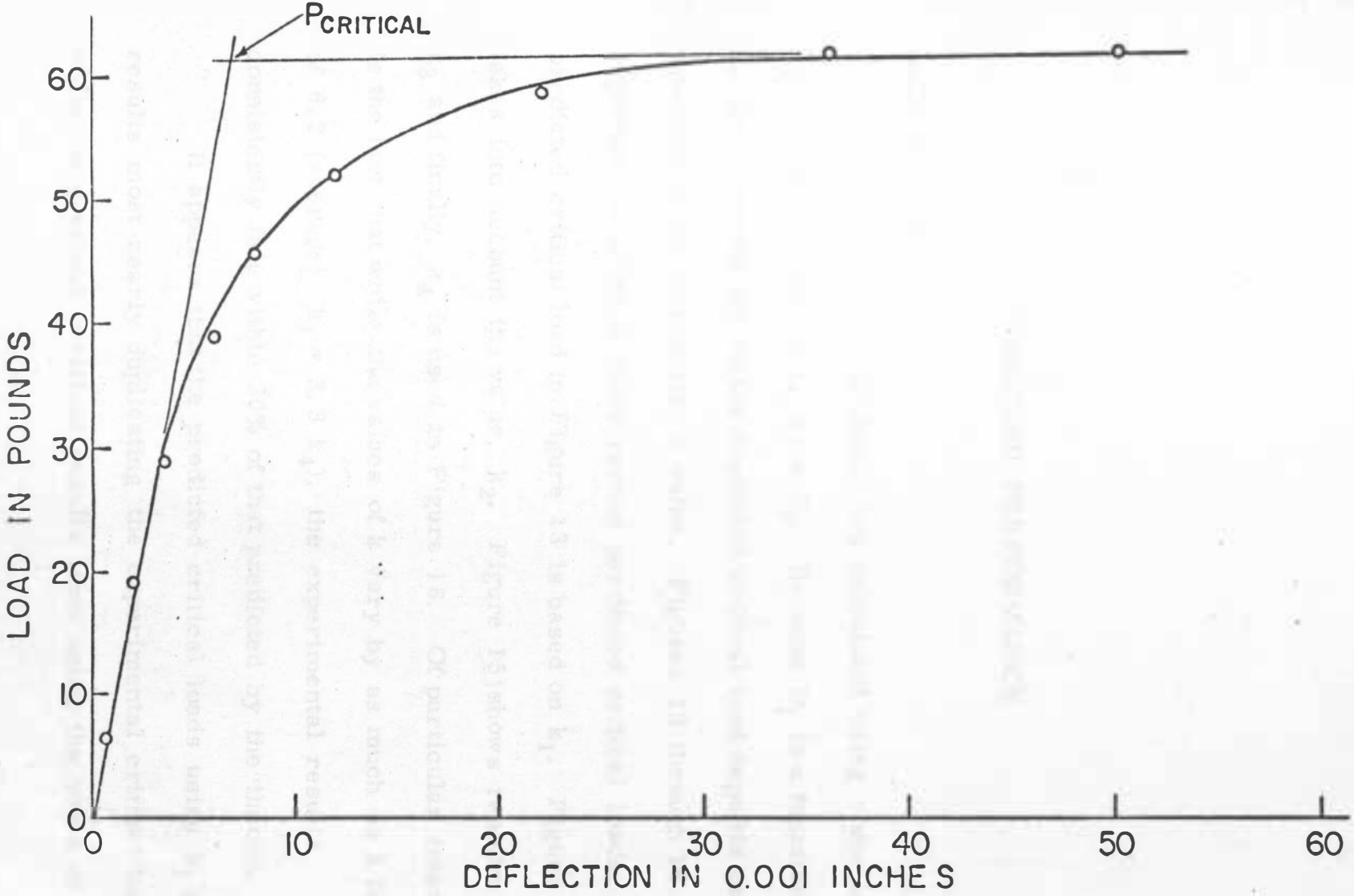

FIGURE 12. LOAD vs DEFLECTION FOR A TYPICAL MODEL PILE TEST

OBSERVED PERFORMANCE

Cohesive Soil

Predicted critical loads are calculated using some length, L_e, which is equal to L_u plus D_f. Because D_f is a function of k, the dependability of the predicted critical load depends on the selection of an appropriate k value. Figures 13 through 16 show experimental critical loads versus predicted critical loads. The predicted critical load in Figure 13 is based on k_1. Figure 14 takes into account the value, k_2. Figure 15 shows results using k_3 and finally, k_4 is used in Figure 16. Of particular interest is the fact that while the values of k vary by as much as a factor of 6.2 (average: $k_1 = 3.3\ k_4$), the experimental results consistently fall within 20% of that predicted by the theory.

It appears that the predicted critical loads using k_1 give results most nearly duplicating the experimental critical loads, while the greatest deviation results from using the value of k_4.

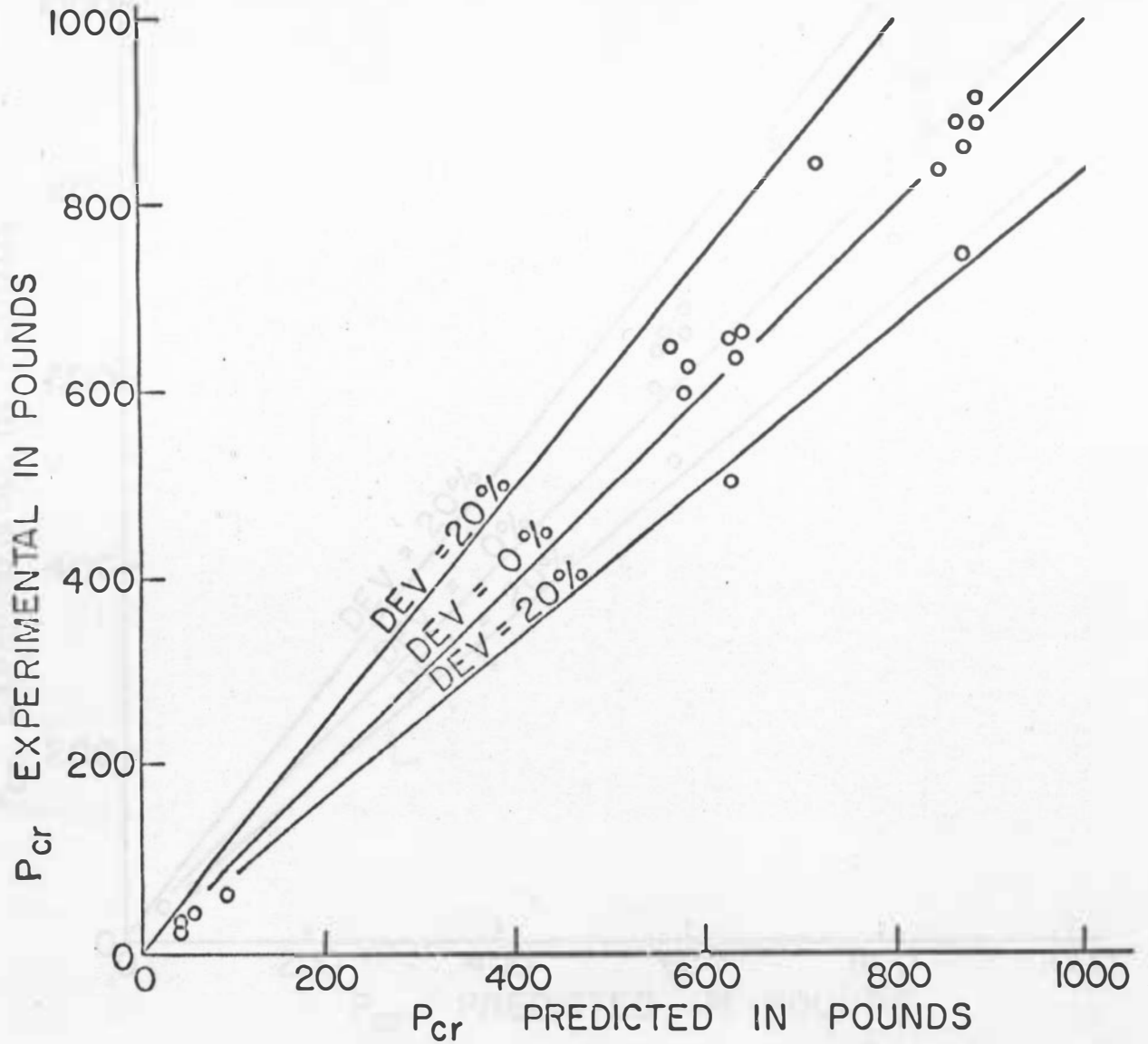

FIGURE 13. P_{cr} EXP vs P_{cr} PRED BASED ON k_1

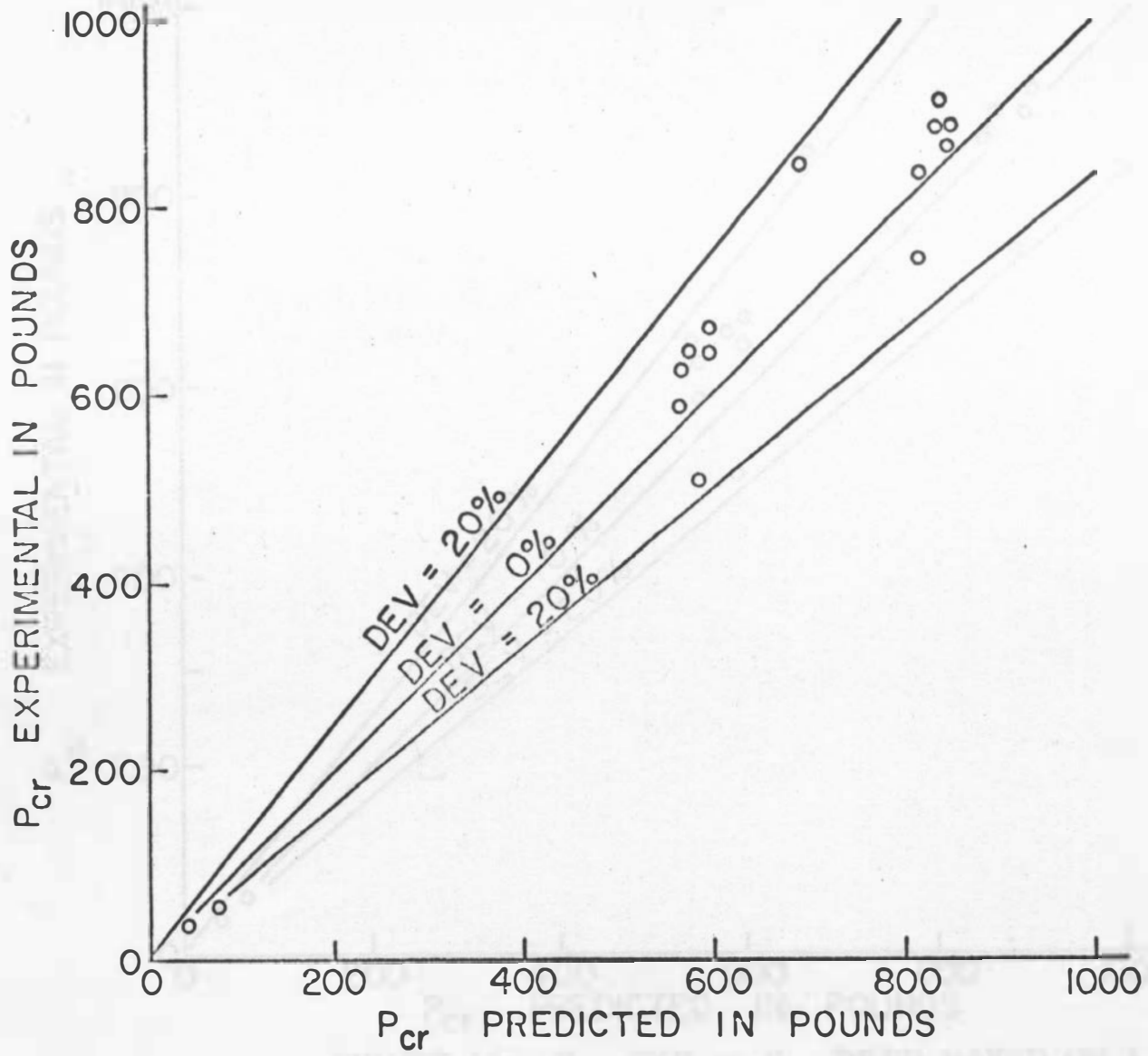

FIGURE 14. P_{cr} EXP vs P_{cr} PRED BASED ON k_2

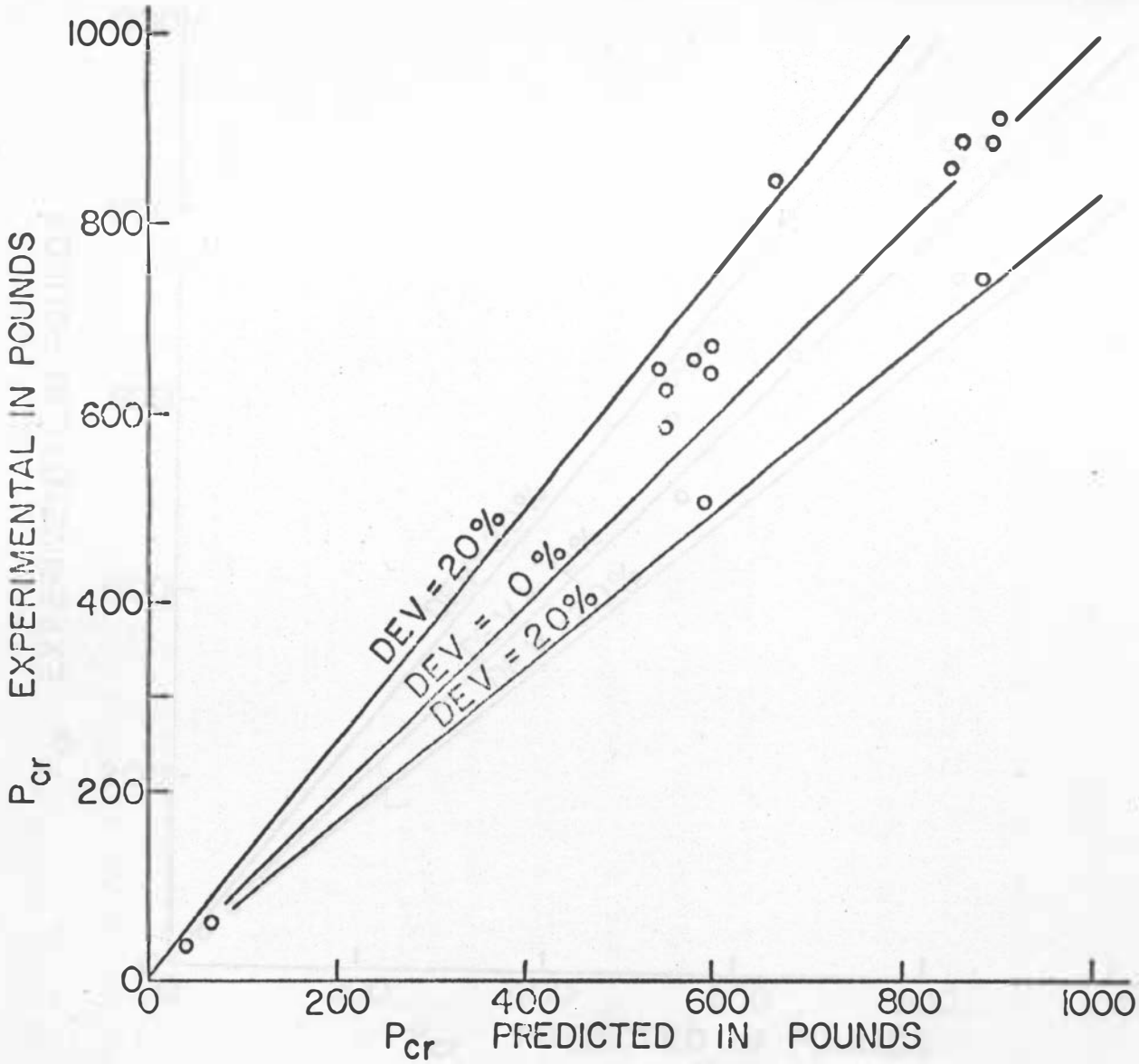

FIGURE 15. P_{cr} EXP vs P_{cr} PRED BASED ON k_3

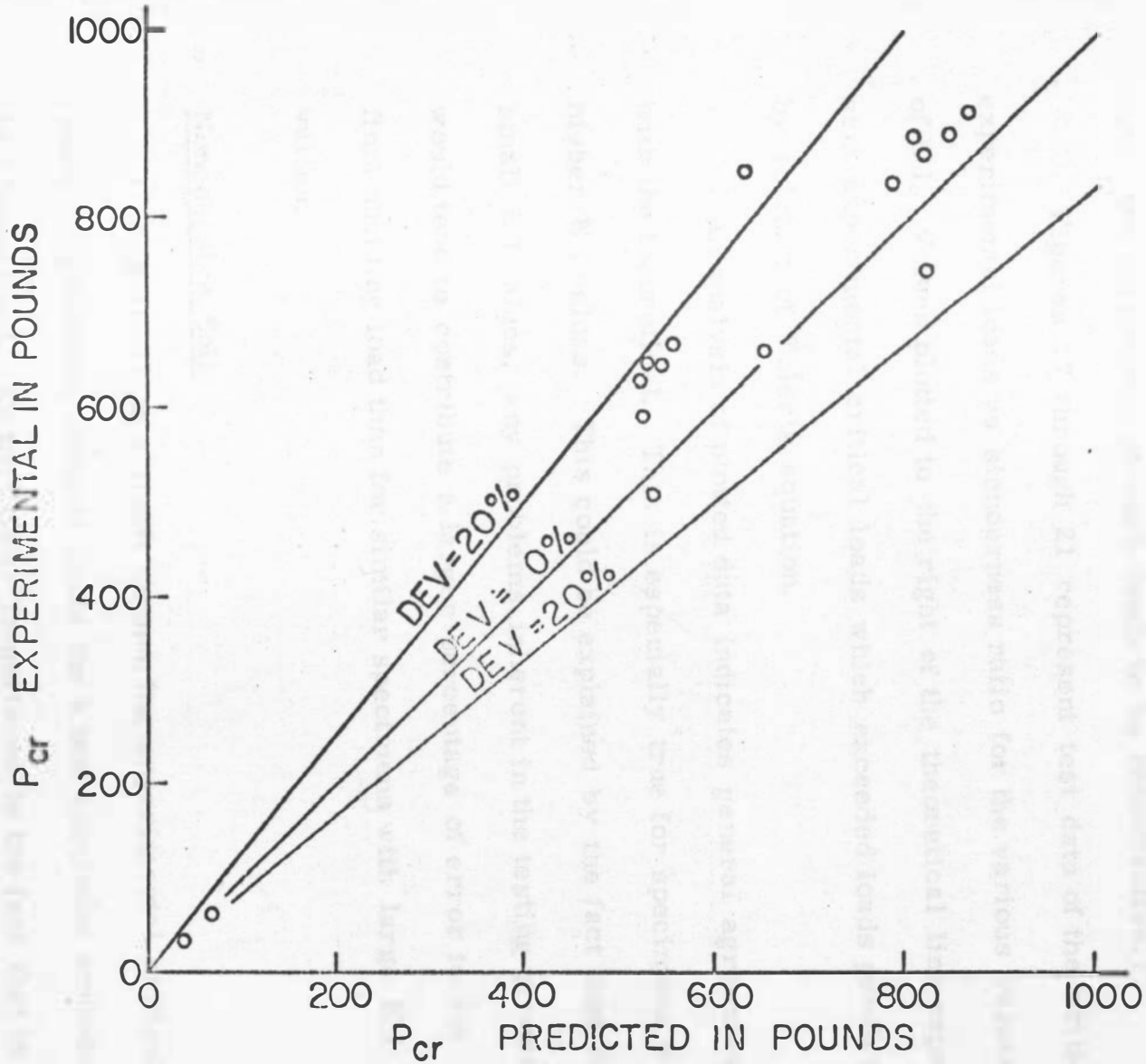

FIGURE 16. P_{cr} EXP vs P_{cr} PRED BASED ON k_4

It should be noted, however, that in nearly all cases, experimental critical loads exceeded the predicted critical loads. (i.e., the analytical approach tends to be conservative.)

Figures 17 through 21 represent test data of the critical experimental loads vs slenderness ratio for the various values of E I. Values plotted to the right of the theoretical line represent experimental critical loads which exceeded loads predicted by solution of Euler's equation.

An analysis of plotted data indicates general agreement with the theoretical. This is especially true for specimens with higher E I values. This could be explained by the fact that for small E I values, any problems inherent in the testing procedure would tend to contribute a larger percentage of error to the final buckling load than for similar specimens with large E I values.

Noncohesive Soil

Figure 22 is a graph comparing experimental critical loads to predicted critical loads for a test specimen embedded in a loose sand. Of particular importance is the fact that in almost all cases, the predicted critical load exceeded the experimental critical load. In a number of cases, the deviation

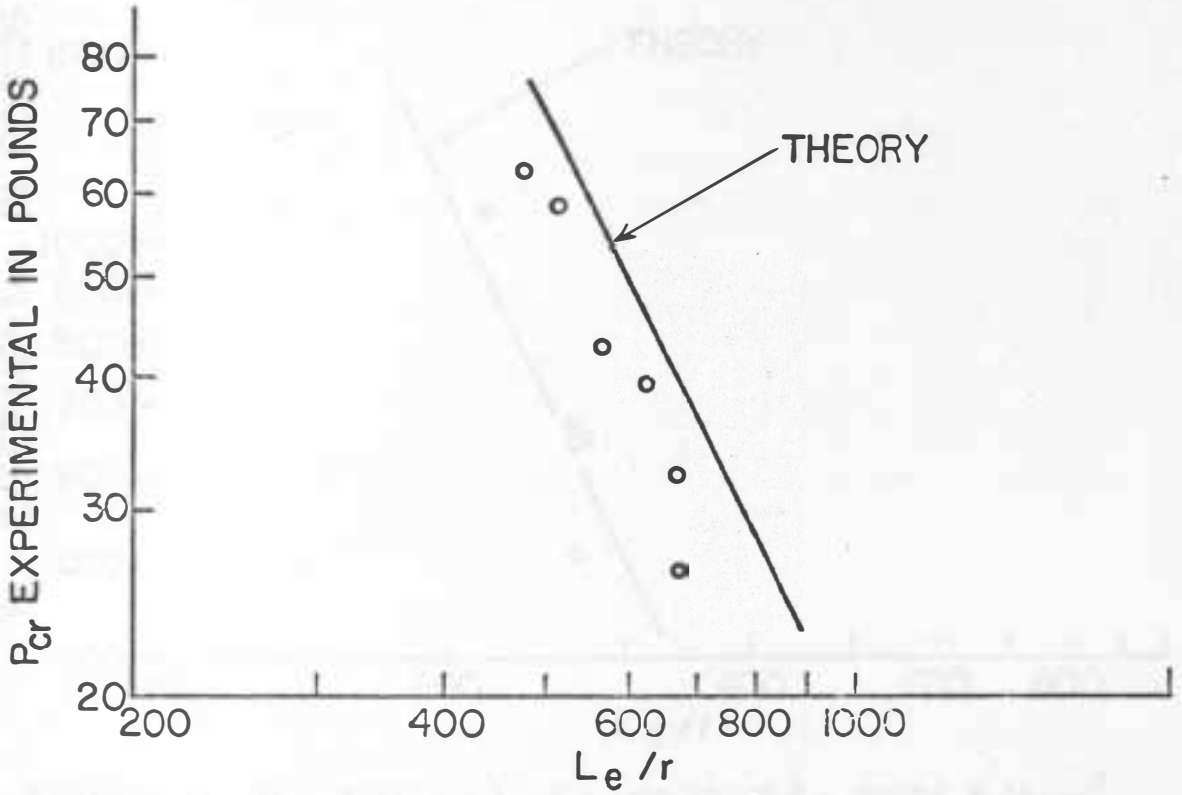

FIGURE 17. P_{cr} EXP vs L_e / r; CLAY; E I = 1820.1 lb-in^2

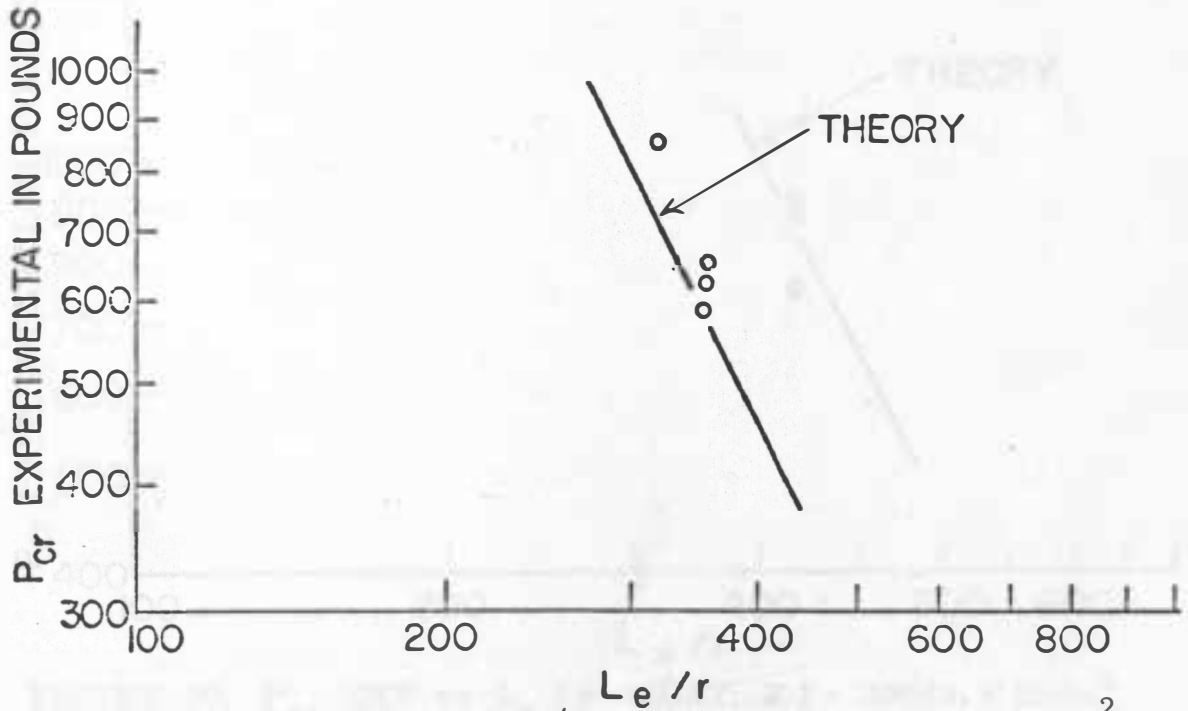

FIGURE 18. P_{cr} EXP vs L_e / r; CLAY; E I = 29322.0 lb-in^2

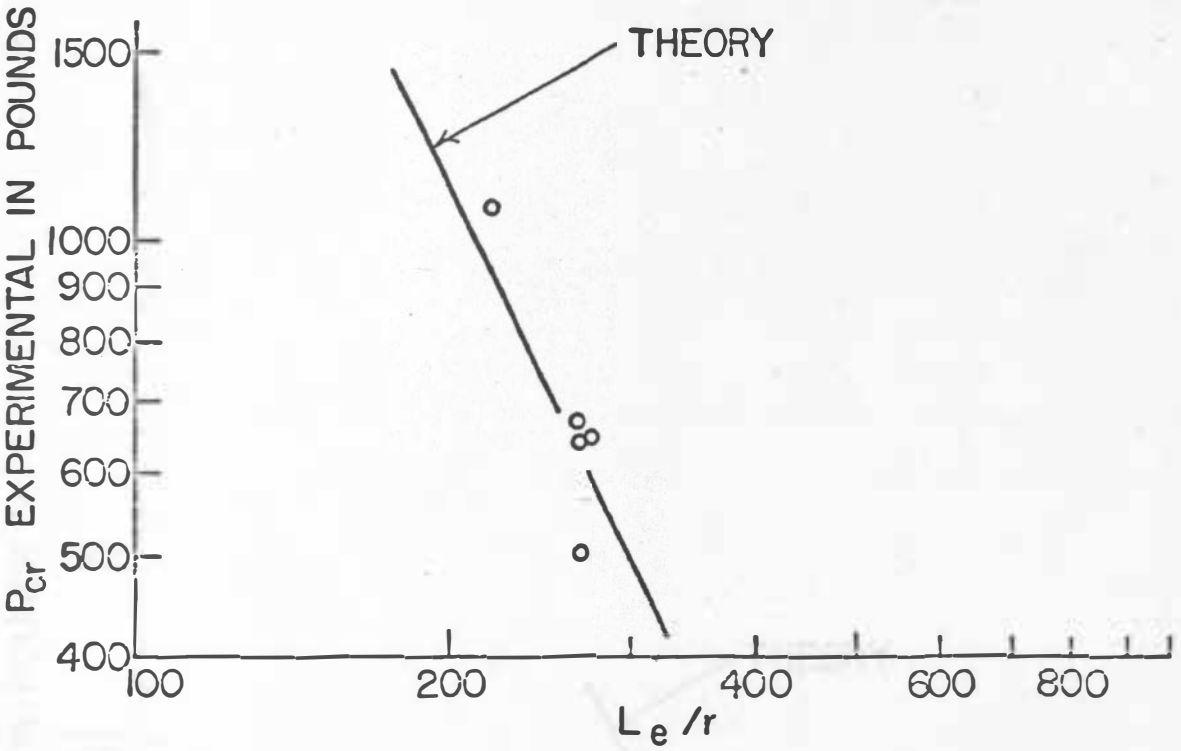

FIGURE 19. P_{cr} EXP vs L_e / r; CLAY; E I = 30383.6 lb-in^2

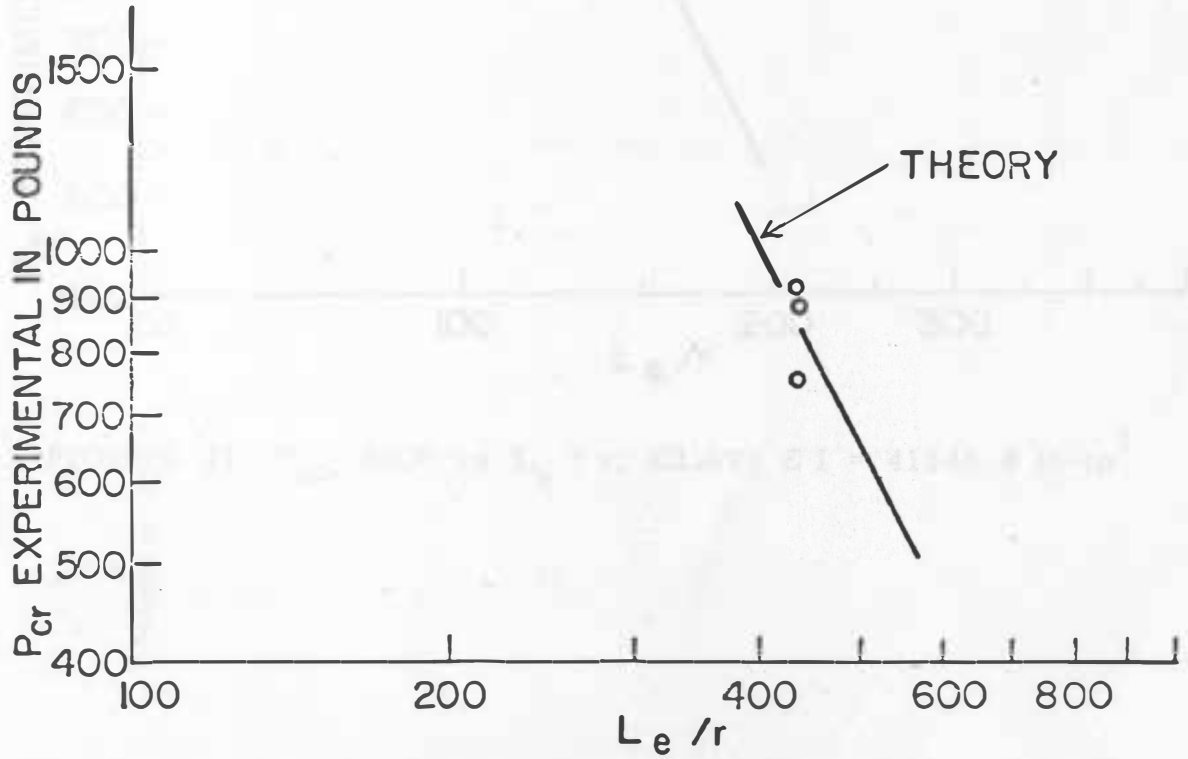

FIGURE 20. P_{cr} EXP vs L_e / r; CLAY; E I = 39062.5 lb-in^2

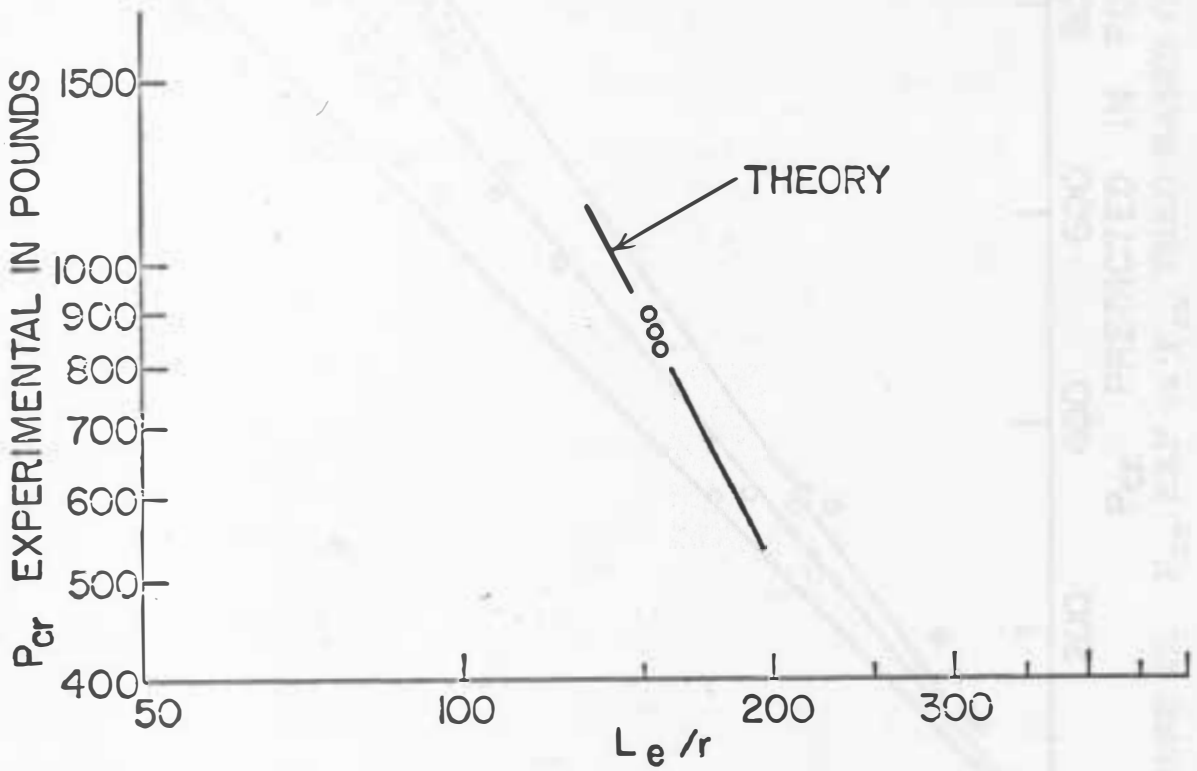

FIGURE 21. P_{cr} EXP vs L_e / r; CLAY; E I = 41348.6 lb-in^2

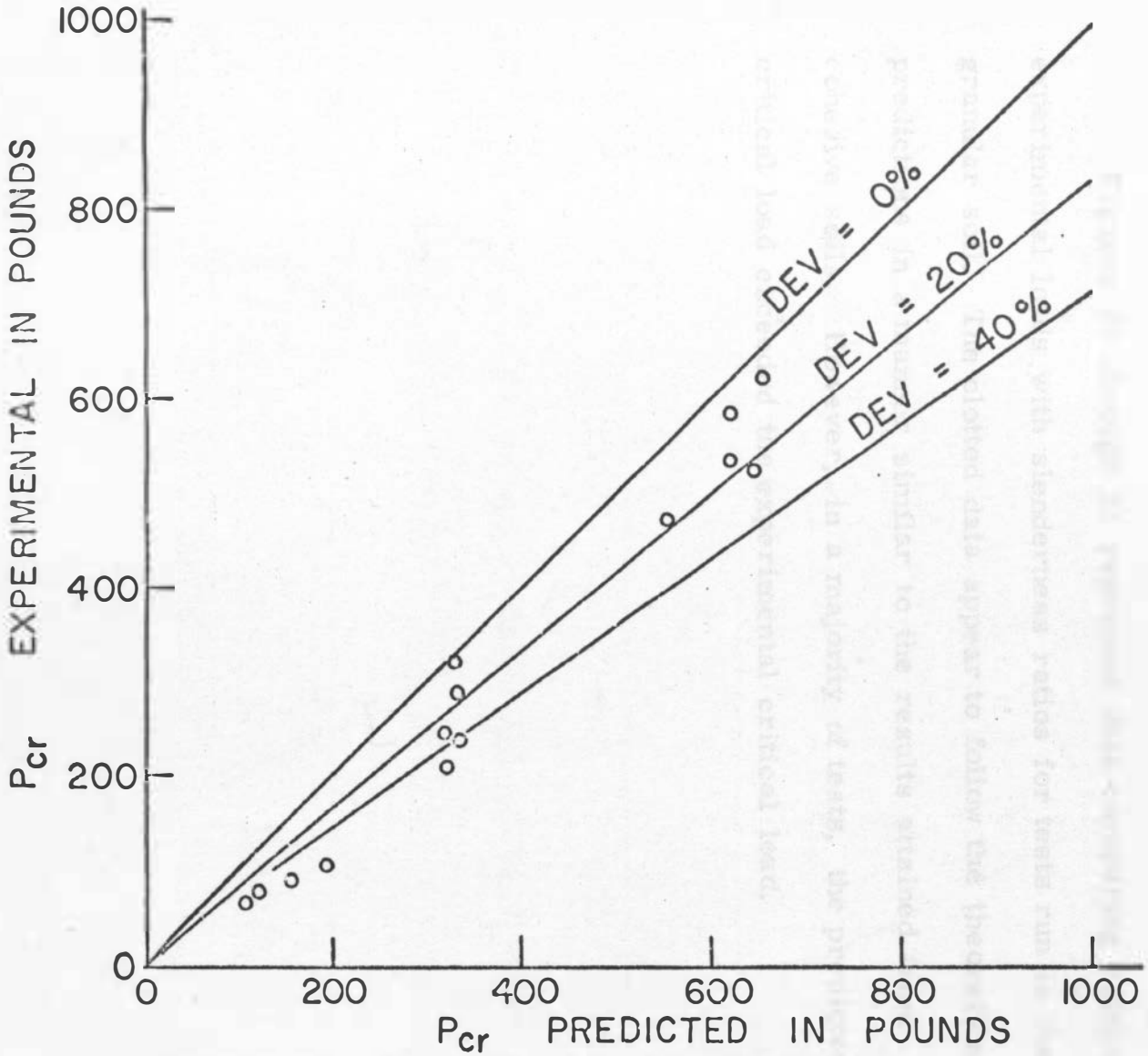

FIGURE 22. P_{cr} EXP vs P_{cr} PRED BASED ON n_H

exceeded 40%. This would suggest that the subgrade modulus value used was too high.

Figures 23 through 25 represent data comparing critical experimental loads with slenderness ratios for tests run in the granular soil. The plotted data appear to follow the theoretical predictions in a manner similar to the results attained from cohesive soils. However, in a majority of tests, the predicted critical load exceeded the experimental critical load.

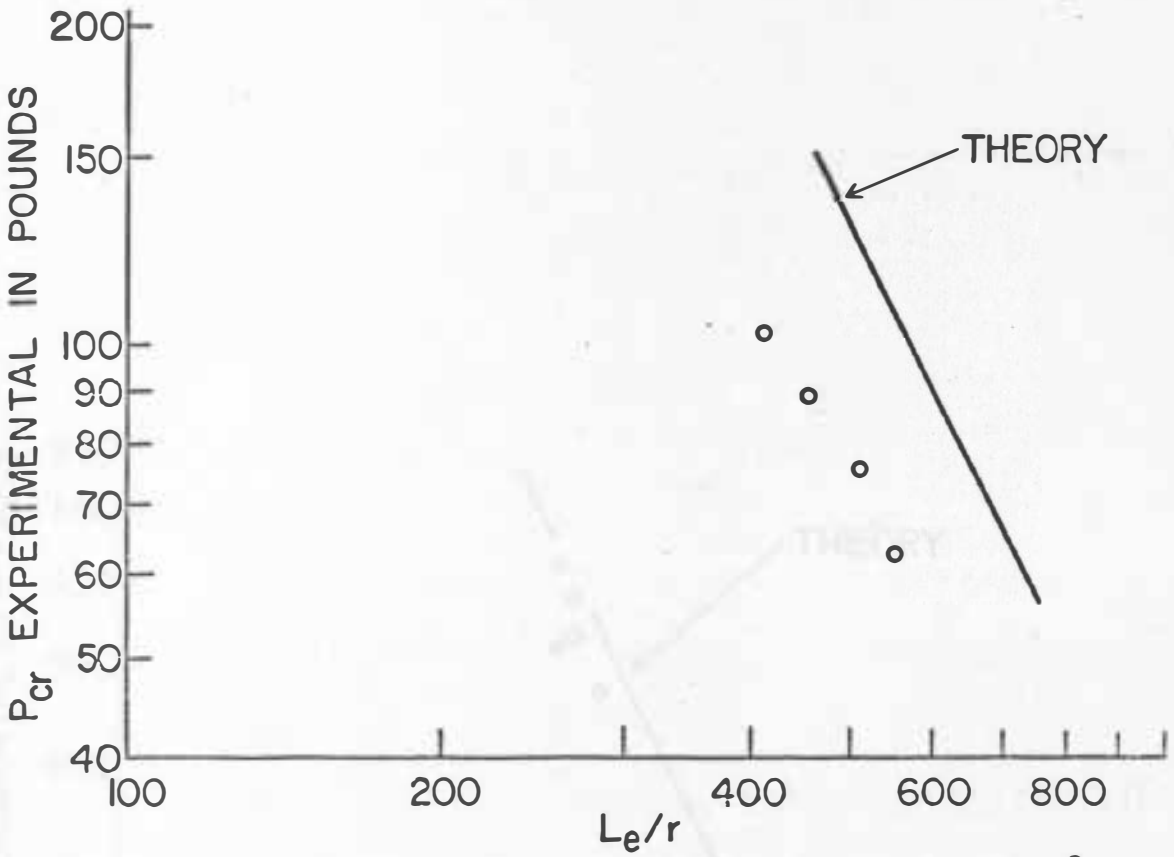

FIGURE 23. P_{cr} EXP vs L_e / r; SAND; E I = 5752.4 lb-in^2

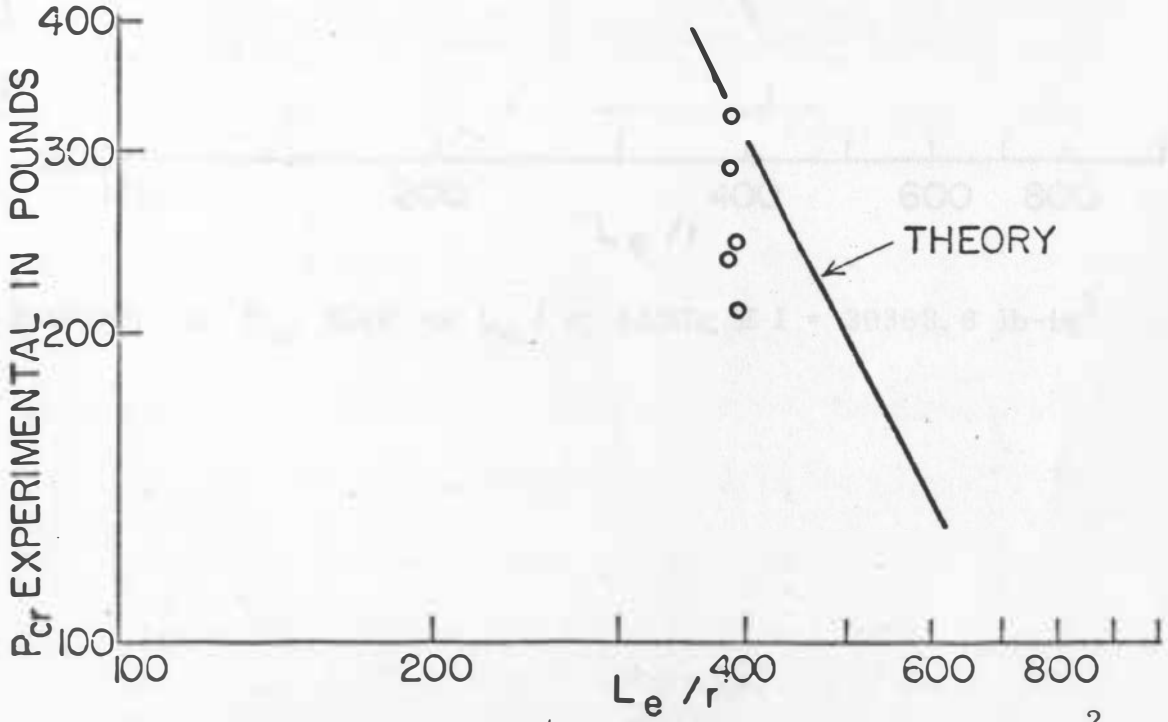

FIGURE 24. P_{cr} EXP vs L_e / r; SAND; E I = 14044.0 lb-in^2

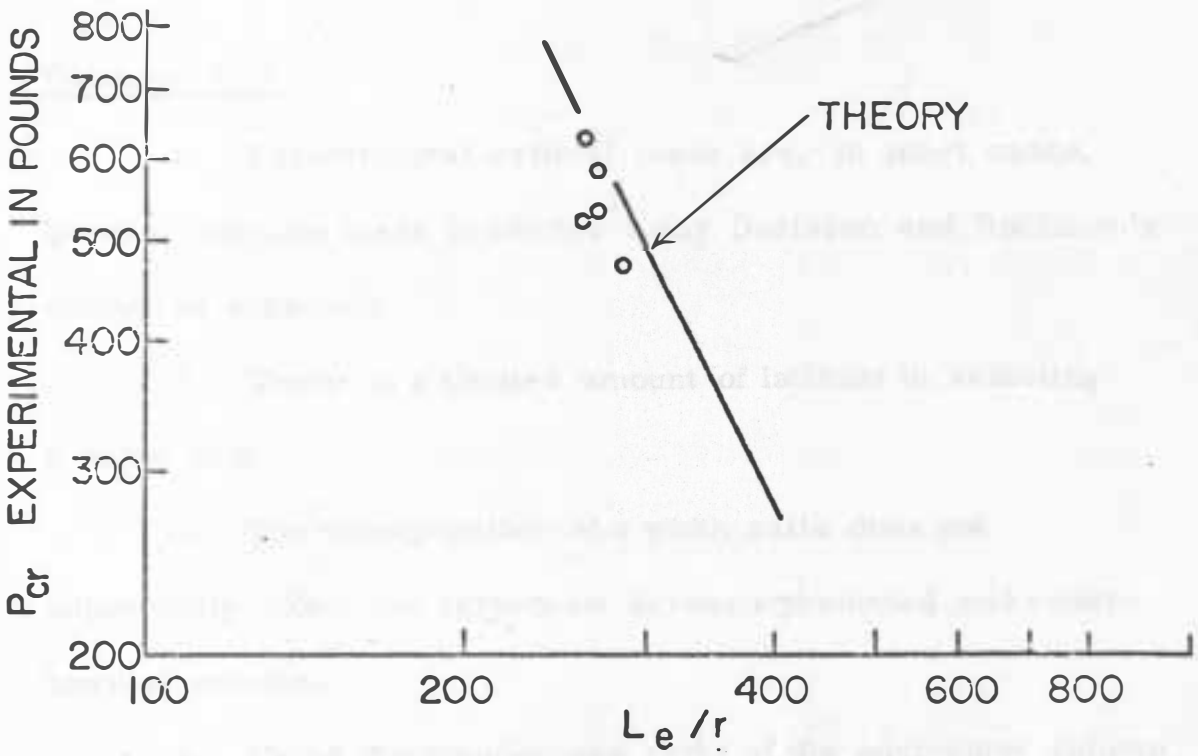

FIGURE 25. P_{cr} EXP vs L_e / r; SAND; E I = 30383.6 lb-in^2

CONCLUSIONS

Cohesive Soil

1. Experimental critical loads are, in most cases, greater than the loads predicted using Davisson and Robinson's analytical approach.

2. There is a limited amount of latitude in selecting a value of k.

3. The incorporation of a width ratio does not appreciably affect the agreement between predicted and experimental results.

4. Using the slenderness ratio of the equivalent column (L_e / r) in conjunction with Euler's buckling equation appears to be a valid means of predicting approximate buckling loads.

5. The testing procedure used does not appear to be as applicable to smaller specimens as it is to larger specimens.

Noncohesive Soil

1. Experimental critical loads are, in most cases, less than the loads predicted using Davisson and Robinson's analytical method.

2. Using the slenderness ratio of the equivalent column (L_e / r) in conjunction with Euler's buckling equation appears to be a valid means of predicting approximate buckling loads.

3. The testing procedure used does not appear to be as applicable to smaller specimens as it is to larger specimens.

RECOMMENDATIONS FOR FURTHER STUDY

1. Model tests should be performed on piles partially embedded in silty soil.

2. An attempt should be made to compare test results from model tests in preloaded clays to model tests in normally loaded clays.

3. The experiment should be extended to include model piles having slenderness ratios ranging from 105 to 300.

4. Tests should be performed on piles approaching the size of typical prototypes.

5. The analytical approach should be extended to include piles of variable cross-section (tapered and step tapered).

6. Model tests should be performed on piles of variable cross-section (tapered and step tapered).

7. Strain gages should be utilized to determine stress patterns and points of flexure in that portion of the pile which is embedded in soil.

8. Model tests should be performed on piles with various types of upper end conditions.

LITERATURE CITED

1. Davisson, M. T. and Robinson, K. E., "Bending and Buckling of Partially Embedded Piles, Proceedings, 6th International Conference of Soil Mechanics and Foundation Engineering, Montreal, 1965, Vol. 2, pp. 243-246.

2. Klohn, E. J. and Hughes, G. T., "Buckling of Long Unsupported Timber Piles," Journal of the Soil Mechanics and Foundation Division, ASCE, Vol. 90, No. SM6, November, 1964, pp. 107-123.

3. Davisson, M. T., discussion of reference 2, Journal of the Soil Mechanics and Foundation Division, ASCE, Vol. 91, No. SM4, July, 1965, pp. 224-225.

4. Lee, Kenneth L., "Buckling of Partially Embedded Piles in Sand," Journal of the Soil Mechanics and Foundation Division, ASCE, Vol. 94, No. SM1, January, 1965, pp. 255-270.

5. Timoshenko, S. P. and Gere, J. M., Theory of Elastic Stability, McGraw-Hill Book Company, Inc., New York, 1936, pp. 204-238.

6. Rocha, M., "The Possibility of Solving Soil Mechanics Problems by the Use of Models," Proceedings, 4th International Conference on Soil Mechanics and Foundation Engineering, London, 1957, Vol. 1, pp. 183-188.

7. Terzaghi, K., "Evaluation of Coefficients of Subgrade Reaction," Geotechnique, Vol. 5, November, 1955, pp. 297-326.

8. Davisson, M. T., "Estimating Buckling Loads For Piles," Proceedings, 2nd Pan American Conference on Soil Mechanics and Foundation Engineering, Sao Paulo, Brazil, July, 1963, Vol. 1, pp. 351-371.

9. Hetenyi, M., Beams on Elastic Foundations, University of Michigan Press, Ann Arbor, 1946.

10. Arges, K. P. and Palmer, A. E., Mechanics of Materials, McGraw-Hill Book Company, Inc., New York, 1963, pp. 308.

APPENDIX A. NOTATION

The following symbols are used in this paper:

A	=	cross sectional area	L^2
B	=	ratio of pile width to width of bar used to determine k	dimensionless
C	=	constant dependent on end conditions of a pile	dimensionless
D_f	=	depth to fixity	L
E	=	modulus of elasticity	FL^{-2}
EI	=	pile stiffness	FL^2
I	=	moment of inertia	L^4
J_R	=	dimensionless unsupported length of pile above ground for pile in clay	dimensionless
J_T	=	dimensionless unsupported length of pile above ground for pile in sand	dimensionless
k	=	modulus of subgrade reaction	FL^{-2}
L	=	embedded length of pile	L
L_e	=	length of equivalent fixed base column	L

L_u	=	unrestrained length of pile	L
l	=	length of equivalent cantilever pile	L
l_{max}	=	dimensionless length of pile below ground for clay	dimensionless
M	=	moment load	FL
n_H	=	constant of horizontal subgrade reaction for granular soils	FL^{-3}
P	=	axial load	F
P_{cr}	=	critical buckling load	F
P_{cr} EXP	=	experimental critical buckling load	F
P_{cr} PRED	=	predicted critical buckling load	F
p	=	lateral force per unit length of pile	FL^{-1}
Q	=	lateral load	F
R	=	nondimensionalizing parameter for clay	L
r	=	radius of gyration	L
S_R	=	dimensionless depth to fixity for clay	dimensionless
S_T	=	dimensionless depth to fixity for sand	dimensionless
T	=	nondimensionalizing parameter for sand	L

U	=	dimensionless axial load for clay	dimensionless
U_{cr}	=	dimensionless critical buckling load for clay	dimensionless
V	=	dimensionless axial load for sand	dimensionless
x	=	depth coordinate	L
y	=	lateral deflection	L
z_{max}	=	dimensionless length of pile below ground for sand	dimensionless

APPENDIX B. TYPICAL VALUES OF k FOR PRELOADED CLAYS

Consistency	Unconfined compressive strength in tons per foot^2	Range of k in pounds per inch^2	Probable value of k in pounds per inch^2
Medium	0.2 - 0.4	100 - 600	110
Stiff	1 - 2	463 - 926	694
Very stiff	2 - 4	926 - 1852	1390
Hard	4	1852	2780

APPENDIX C. TYPICAL VALUES OF n_H

Soil Type	n_H in pounds per inch^3	
	Dry	Submerged
Sand:		
Loose	9.4	5.3
Medium	28	19
Dense	75	45
Very loose, under repeated loading		1.5
Silt:		
Very soft, organic		0.4 - 1.0
Clay:		
Very soft		
static loads		2
repeated loads		1

APPENDIX D. COHESIVE SOIL CLASSIFICATION DATA

Classification based on Unified system: Silty CLAY, CL

Percent passing 200 sieve	60.4%
Liquid Limit	26.3%
Plastic Limit	18.7%
Plastic Index	7.6%

Proctor Density: 126.6 pounds per foot^3

Optimum Moisture 10.5%

Average density during tests: 115.3 pounds per foot^3

Average moisture content during tests 15.2%

APPENDIX E. NONCOHESIVE SOIL CLASSIFICATION DATA

Classification based on Unified system:	SAND, SP
Percent passing 4 sieve	100.0%
Percent passing 200 sieve	0.5%
D_{10}	0.20mm
D_{60}	0.67mm
C_U	3.35

Density at maximum void ratio: 101.3 pounds per foot^3

Density at minimum void ratio: 112.0 pounds per foot^3

Relative density during testing 0.0%